Improved forest dynamics leads to better hydrological predictions in watershed modeling

ABSTRACT

This study explored how the characterization of forest processes in hydrologic models affects watershed hydrological responses. To that end, we applied the widely used Soil and Water Assessment Tool (SWAT) model to two forested watersheds in the southeastern United States. Although forests can cover a large portion of watersheds, tree attributes such as leaf area index (LAI), biomass accumulation, and processes such as evapotranspiration (ET) are rarely calibrated in hydrological modeling studies. The advent of freely and readily available remote-sensing data, combined with field observations from forestry studies and published literature, allowed us to develop an improved forest parameterization for SWAT. We tested our proposed parameterization at the watershed scale in Florida and Georgia and compared simulated LAI, biomass, and ET with the default model settings. Our results showed major improvements in predicted monthly LAI and ET based on MODIS reference data (*NSE* > 0.6). Simulated forest biomass also showed better agreement with the USDA forest biomass gridded data. Through a series of modeling experiments, we isolated the benefits of LAI, biomass, and ET in predicting streamflow and baseflow at the watershed level. The combined benefits of improved LAI, biomass, and ET predictions yielded the most optimal model configuration where terrestrial and in-stream processes were simulated reasonably well. We performed automated model calibration using two calibration strategies. In the first calibration scheme (M_0), SWAT was calibrated for daily streamflow without adjusting LAI, biomass, and ET. In the second calibration scheme ($M_{LAI+BM+ET}$), previously calibrated parameters constraining LAI, biomass, and ET were incorporated into the model and daily streamflow was recalibrated. The $M_{LAI+BM+ET}$ model showed superior performance and reduced uncertainties in predicting daily streamflow, with *NSE* values ranging from 0.52 to 0.8. Our findings highlight the importance of accurately representing forest dynamics in hydrological models.

KEYWORDS: SWAT, Forest dynamics, Watershed hydrologic modeling, Leaf area index, Evapotranspiration, Biomass, MODIS

1. INTRODUCTION

Any ecosystem in a watershed affects the quantity and quality of the water passing through it by either improving or degrading the hydrologic services (Brauman et al., 2007). For example, forested ecosystems might increase rainfall infiltration rates while decreasing water yield (Filoso et al., 2017). This is mainly due to the higher water infiltration capacity of forest soils compared to other land uses (Bruijnzeel, 2004). Since forests can make up large portions of a watershed system, it is important to understand their role in the hydrologic cycle and how they influence the pathways and distribution of water in the watershed (Amatya el al., 2015). Forests can tightly interact with the hydrologic cycle through the canopy interception of precipitation; the redistribution of water via throughfall, stemflow, surface runoff, lateral flow, soil infiltration, percolation, groundwater recharge and baseflow; and the loss of water by soil evaporation and transpiration from foliage. Thus, through the use, transport, and partitioning of water, forest ecosystems can significantly alter the volume and timing of water reaching downstream locations (Brauman et al., 2007).

In recent years, there has been a growing interest in investigating the interface between watershed vegetation and hydrologic processes (Amatya et al., 2015; Hernandez et al., 2018; Sun et al., 2005; Williams et al., 2012; Wit, 2001). As water yield from forestlands is critical for supporting ecosystem biodiversity and local communities, there is an urgent need to better understand the nexus between forests and water in order to orient science-based sustainable watershed development (Amatya et al., 2015; Brown et al., 2016; Sun et al., 2005). Watershed-scale hydrological models have been successfully employed to investigate the interactions among forests and components of the hydrological cycle (Brown et al., 2015; Golden et al., 2016; Ziemer et al., 1991). A hydrological model capable of accounting for the spatial and temporal variability

of factors affecting hydrological processes (e.g., intra-annual plant growth cycle, landscape heterogeneity) is a useful tool for understanding, predicting, and managing water resources (Khaki et al., 2019; Loizu et al., 2018; Zhang et al., 2019). In this context, reliable watershed models that can realistically represent forest-water relationships can be powerful tools.

An accurate representation of the simulated system is critically important for the performance of hydrological models in predicting a given target variable (Jiang and Wang, 2019). Even though forests can regulate water cycling and significantly affect water fluxes within a watershed, watershed modelers rarely pay attention to the accuracy of their representation in capturing forest attributes and processes such as leaf area index (LAI), biomass, and evapotranspiration (ET). Streamflow is usually selected as the only variable to measure the performance of watershed models since streamflow data are relatively easy to obtain (Li Zejun et al., 2020). The information contained in gauged streamflow data may not sufficiently capture vertical fluxes and how they vary in space and time within the watershed (Rajib et al., 2018), thus leading to inaccurate representation of relative contributions of various fluxes. For instance, hydrological fluxes such as infiltration, soil evaporation, plant transpiration, and evapotranspiration evolve at different spatial and temporal scales within a watershed and affect the water balance (Tague and Band, 2001). Streamflow data lumps horizontal water movement (i.e., runoff) and vertical water fluxes (e.g., evapotranspiration) together (Li Zejun et al., 2020), thus leading to inaccurate representation of horizontal and vertical fluxes. This may lead to erroneous conclusions if the model is used to assess, for example, the impacts of forest management practices (e.g., thinning, fertilization) or deforestation/afforestation on water resources. Also, forestlands can modify soil hydraulic conductivity, porosity, capillarity, and texture (e.g., increased organic

matter content), having underlying effects on soil water infiltration, subsurface flows, and groundwater flows (Tabacchi et al. 2000).

The Soil and Water Assessment Tool (SWAT) (Arnold et al., 1998) has been extensively applied worldwide to estimate water yield (Abou Rafee et al., 2019; Adla et al., 2019; Kaur et al., 2019), sediment loss (Wang and Kalin, 2018; Brighenti et al., 2019; Himanshu et al., 2019; Mishra et al., 2007), nutrient loading (Ramesh et al., 2020; Akhavan et al., 2010; Chu et al., 2004; Haas et al., 2016), and assess the impacts of climate (Dosdogru et al., 2020; Ahn et al., 2016; Anjum et al., 2019; Awan and Ismaeel, 2014) and land use/cover changes (Anand et al., 2018; Haas et al., 2021a; Jodar-Abellan et al., 2018; Li et al., 2014; Romanowicz et al., 2005; Teklay et al., 2019; Wang et al., 2018) on water resources.

SWAT has not been sufficiently tested in forested ecosystems yet (Yang et al., 2018) and had shown some limitations to accurately simulate plant growth (Zhang et al., 2020), especially LAI development. To address these issues, a few studies have been carried out to revise SWAT's plant database. For example, Strauch and Volk (2013) proposed a new plant growth approach based on changes in soil moisture for tropical regions and presented a logistic LAI decline function. Similarly, Alemayehu et al. (2017) presented a quotient of rainfall and reference evapotranspiration to initialize the plant growth cycle in SWAT. The authors tested the methodology for a variety of land uses in Kenya and Tanzania and showed improvements in simulated LAI based on remote-sensing derived data. Yang and Zhang (2016) identified unrealistic parameter values representing evergreen forests, deciduous forests, and mixed forests in SWAT and proposed an improved model parameterization tested at ten Ameriflux sites. Yang et al. (2018) extended the previous study to the watershed scale and showed positive effects for streamflow prediction. Watson et al. (2005) replaced the original SWAT plant growth model with the 3-PG

95 forest growth model to better represent the growth of *Eucalyptus* trees in Australia. More recently,
96 Lai et al. (2020) presented a forest growth model featuring variable density and mixed vegetation
97 types in SWAT. Their results showed that the modified model outperformed the original model in
98 simulating flow and nutrient load.

99 Although all these studies offer valuable insights and potential contributions to the
100 modeling community, they fall into oversimplifications (e.g., lumped forest types), insufficient
101 representation of plant growth components (e.g., LAI + biomass + ET), an excessive amount of
102 input data (e.g., forest growth data required by 3-PG), and lack of demonstration of the extents to
103 which forest processes affect the watershed hydrology. To the best of the author's knowledge, no
104 study in the literature demonstrated the watershed-scale benefits of realistically representing forest
105 attributes in watershed modeling. Most of the modeling studies found in the literature lumped
106 parameters for groups of forests and thus did not consider underlying characteristics of specific
107 forest types, such as pines. In forested regions such as the southeastern U.S., for example, where
108 specific pine species like loblolly pine (*Pinus taeda L.*) and slash pine (*Pinus elliottii*) dominate
109 the landscape, it is necessary to better test SWAT's skills and tune the model to better represent
110 these tree species.

111 Considering that forests can cover large portions of watersheds and greatly interfere with
112 the hydrological cycle and that SWAT has been widely applied as a hydrological prediction and
113 assessment tool, it is fundamental to understand and evaluate the model's skills in forested
114 ecosystems. LAI and biomass, besides being key forest attributes representing forest growth and
115 dynamics, play important roles in SWAT's hydrological computations. For instance, LAI affects
116 plant transpiration, canopy rainfall storage, and evapotranspiration (if the Penman-Monteith
117 method is used to simulate ET) in SWAT (Neitsch et al., 2011). Likewise, aboveground biomass

and soil residue affect soil evaporation rates in the model. SWAT's semi-distributed characteristic capable of discretizing the landscape into smaller units combined with the vast amount of freely available remote-sensing data presents a great opportunity for modelers to step forward from the traditional modeling calibration approach (i.e., streamflow only) and incorporate additional constraints into the models. A large number of studies have reported the benefits of using remote-sensing derived data to increase the accuracy of watershed models (Gui Ziling et al., 2019; Ha et al., 2018; Herman et al., 2018; Jiang and Wang, 2019; Ma et al., 2019; Odusanya et al., 2019; Parajuli et al., 2018; Rajib et al., 2016; Tobin and Bennett, 2017; Y. Zhang et al., 2020). In a recent effort, Haas et al. (2021b) developed an improved SWAT re-parameterization of forest processes and tested it for loblolly pine and slash pine, the two major pine species in the southeastern United States. The methodology was based on remote-sensing data combined with field observations and was successfully tested at different field-scale sites across the southeastern United States. Although the developed re-parameterization outperformed the default model in predicting tree LAI, biomass, and ET, the hydrological implications at the watershed scale were not investigated.

Therefore, the overreaching goal of this study was to investigate the importance of accurately capturing forest processes in watershed-scale hydrological models and assess their implications for simulated discharge and water balance computation. Our specific objectives were to: (1) assess the feasibility of transferring previously calibrated biophysical parameters to two forested watersheds; (2) determine which forest attributes and processes (LAI development, biomass accumulation, or ET rates) affect streamflow and water budget the most; and (3) assess the effects of multi-facet model calibration (LAI + biomass + ET + streamflow) on streamflow prediction compared to traditional model calibration (streamflow only). It is hypothesized that an enhanced representation of forest dynamics in SWAT will positively affect its performance in

141 simulating streamflow due to a more realistic prediction of leaf area development, canopy storage,
142 and precipitation lost as ET. The novelty of this study is in demonstrating the effect of forest
143 dynamics on hydrological processes using a ready-to-go improved model parameterization based
144 on open-source remote sensing products, published literature, and shared field observations. Such
145 level of detail and reflection of real-world interplays of natural processes (i.e., water, energy,
146 vegetation) could never be achieved through traditional model calibration against streamflow only.

147 The remainder of the paper is organized as follows: In section two, we describe the study
148 area, the watershed model utilized, the modeling scenarios designed to assess the importance of
149 forest processes in hydrologic predictions, and the statistical analyses employed to evaluate the
150 model performance. In section three, we present the results, discuss, and interpret them in light of
151 the published literature, highlight some limitations of our study, and suggest future directions
152 related to the incorporation of forest growth and dynamics in watershed models. Finally, in section
153 four, we summarize our main findings and stress their implications in applying watershed models
154 as tools to support decision-making.

155 ## 2. MATERIAL AND METHODS

156 ### 2.1.Study sites

157 The Upatoi Creek and Upper Santa Fe River watersheds located in Florida and Georgia,
158 respectively, were selected as the study sites (Fig. 1). These watersheds were suitable to test our
159 hypothesis that a better simulation of key forest processes can result in better streamflow prediction
160 because both are highly forested in either loblolly or slash pine tree species. Both have long-term
161 daily streamflow records. The Upatoi Creek Watershed (UCW) is in Chattahoochee County, near
162 Columbus, Georgia, and has a drainage area of approximately 900 km^2. Upatoi Creek is a 57 km
163 long river running from South Columbus to the Chattahoochee River. The elevation ranges from

73 to 255 meters in the watershed, and according to the Soil Survey Geographic Database (SSURGO), there are 172 different soil classes at UCW, out of which 75 are hydrological soil group (HSG) A, 47 are HSG B, and 50 are HSG C. The land use and cover at UCW are mainly dominated by loblolly pine trees (57%) and shrubs (9%).

The Upper Santa Fe River Watershed (SFRW) is part of the Santa Fe River Basin system and has a drainage area of approximately 500 km^2 and elevation ranging from 25 to 83 meters. Located predominantly in Union County, Florida, the SFRW is situated approximately 40 km north of the city of Gainesville. In terms of land use and cover, the SFRW is dominated by slash pine trees (56%) and hay-pasture (12%). (Soils in the SFRW are mostly HSG's A and B with a few HSG's C.

Additional Hydrometeorological characteristics portraying both watersheds are summarized in Table 1.

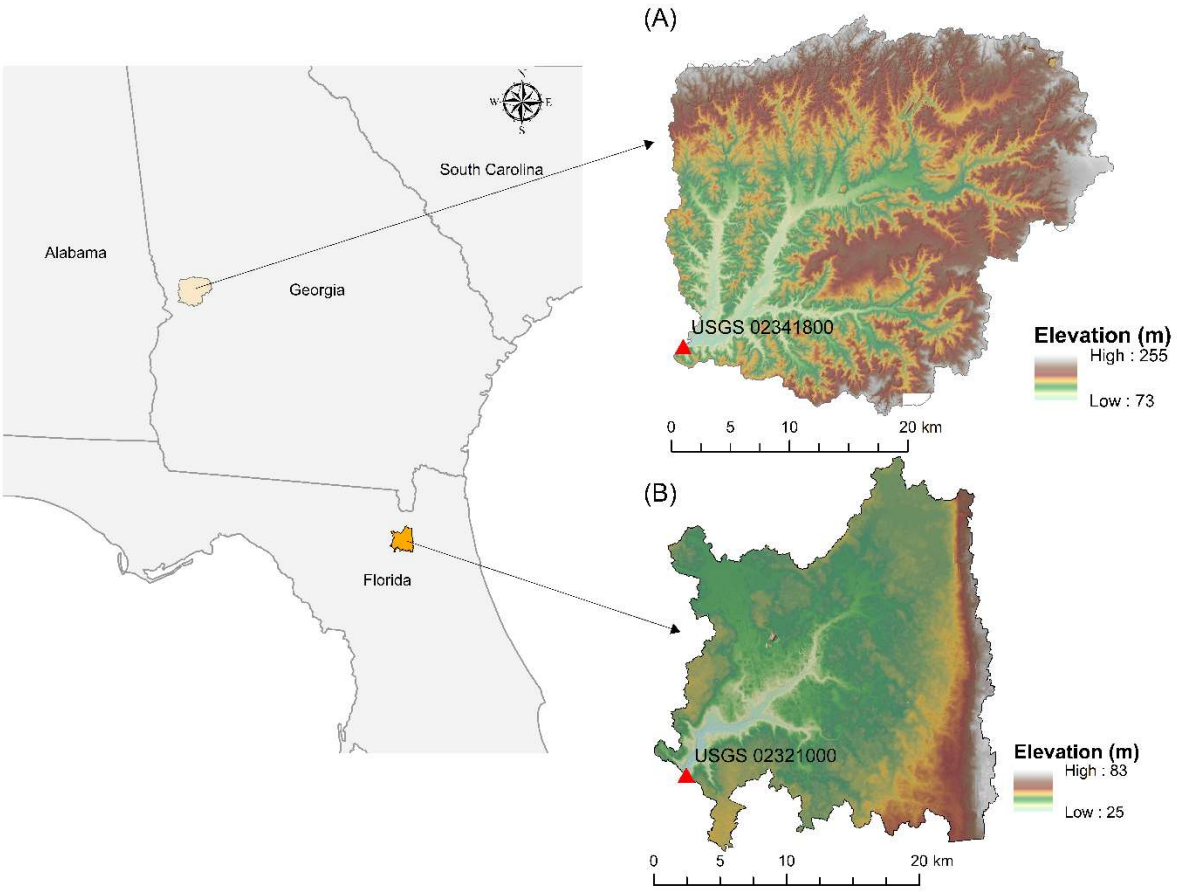

Figure 1. Location map. (A) Upatoi Creek watershed, (B) Upper Santa Fe River watershed.

Table 1. Watershed characteristics

Hydrometeorological variable	Upatoi Creek	Upper Santa Fe
Latitude	32.544, 32.61 N	29.964, 30.165 N
Longitude	-84.811, -84.442 W	-82.247, -82.045 W
Area (km^2)	881.75	487.84
Average mean daily temperature (°C) (1995-2018)	18.2	20.48
Average annual precipitation (mm) (1995-2018)	1295.8	1326.5
Mean annual potential evapotranspiration (mm) (1995-2018)	1268	1215.2
Mean annual discharge (mm)* (2002-2018)	481	314
Mean daily streamflow (m^3/s) (1998-2018)	10.7	3.1

2.2.The SWAT Model

The SWAT hydrological model was used in the current study to investigate the effects of forest dynamics on key hydrological processes within the study watersheds. SWAT is one of the most widely used hydrological models and a well-established tool capable of simulating various water fluxes (e.g., surface runoff, lateral flow, groundwater contribution) and plant growth. Additional model components include weather, transport of sediment, nutrients, bacteria, and pesticides, and land management. SWAT is a watershed-scale, semi-distributed, continuous-time, open-source model developed by the United States Department of Agriculture (USDA) Agricultural Research Service (ARS). The model discretizes a watershed into subwatersheds, which are further discretized into unique combinations of land use, soils, and slope called hydrological response units (HRU's) (Neitsch et al., 2011).

In SWAT, the water balance calculation for each HRU considers five storages: snow, canopy storage, the soil profile with up to ten layers, a shallow aquifer, and a deep aquifer. The water balance is calculated using the following:

$$\Delta S = \sum_{t=1}^{t}(P - Q_{total} - ET - w_{seep}) \quad (1)$$

where, ΔS is the change in water storage, P, Q_{total}, ET, and w_{seep} are the daily amount of precipitation, total water yield, evapotranspiration, and the total amount of water exiting the bottom of the soil profile on a given day, respectively. The value of w_{seep} is a sum of the amount of water percolating out of the lowest soil layer and the amount of water flowing past the lowest boundary of the soil profile due to bypass flow. The total water yield (Q_{total}) represents an aggregated sum of surface runoff, lateral flow, and the base flow contribution to streamflow. In this study, surface runoff was computed using the Soil Conservation Service (SCS) Curve Number

(CN) method based on daily rainfall observations, and the Penman-Monteith (Monteith, 1965) method was selected for estimating evapotranspiration.

SWAT incorporates a simplified version of the Environmental Policy Integrated Climate (EPIC) model (Williams, 1990) to simulate the growth of different types of crops and trees. The initialization of the growth cycle in SWAT is based on the heat unit theory: plants require a certain amount of heat to reach maturity, which is only reached when a plant-specific total heat unit is attained. Once the plant reaches maturity, it stops transpiring and uptake of water and nutrients. In SWAT, the growth cycle restarts every year based on a latitude-dependent dormancy routine or via harvest and kill operation in the model's management module. At the beginning of each growth cycle, the accumulated heat units drop to zero and the LAI is set to a plant-specific minimum value defined by the user (Neitsch et al., 2011). During the early stage of plant growth, SWAT simulates phenological development using an optimal leaf area index development curve. The plant's biomass accumulation is based on canopy light interception and the plant's efficiency in converting intercepted radiation into biomass. For detailed information about SWAT's representation of forest growth and dynamics and how it affects the simulation of hydrological processes, readers are referred to Haas et al. (2021b).

Given SWAT's limitations in simulating tree growth (Lai et al., 2020; Ma et al., 2019; Strauch and Volk, 2013; Yang et al., 2018; Yang and Zhang, 2016), the current study uses the improved model parameterization describing loblolly and slash pine growth and dynamics introduced by Haas et al. (2021b). This improved forest parameterization was developed based on field measured forestry data, remote-sensing estimates of LAI, expert knowledge, and a review of published literature. Further details about SWAT's computation of physical processes can be found in Neitsch et al. (2011).

226 2.3.Model setup and data acquisition

227 As a semi-distributed watershed-scale hydrological model, SWAT requires several geospatial
228 inputs and weather forcing to simulate physical processes within a watershed. The ArcSWAT 2012
229 (version 10.4.19) interface was used in this study to delineate the watersheds and define their
230 respective number of HRU's. First, the watershed's boundaries were delineated based on 10 meters
231 resolution digital elevation model (DEM) from the National Elevation Dataset (NED) and
232 hydrography network from the National Hydrography Dataset (NHD). Soil maps and soil
233 characteristics (e.g., soil depth, soil hydraulic conductivity, available water capacity) needed to
234 parameterize SWAT's soil database were obtained from SSURGO as gridded data covering the
235 watershed's drainage area. A reclassified land use map based on the publicly available 30 meters
236 resolution National Land Cover Database (NLCD) 2016 was ingested in ArcSWAT.

237 The land use reclassification was deemed necessary to capture the spatial distribution of
238 loblolly and slash pine across the watersheds as accurately as possible. Thus, a pre-processing step
239 involving reclassification of NLCD 2016 was conducted using the National Forest Type Dataset
240 (NFTD) (Ruefenacht et al., 2008) as a background map to discretize NLCD's forest classification
241 into species-specific and geographically-meaningful types of trees. NFTD is a publicly available
242 geospatial dataset at 250 meters resolution developed by the United States Forest Service (USFS)
243 Forest Inventory and Analysis (FIA) program and the Geospatial Technology and Applications
244 Center (GTAC). This dataset was created to show the extent, spatial distribution, and forest type
245 composition of forests within the United States territory. We pre-processed this gridded dataset in
246 ArcMap 10.4.1 to make it readable in ArcSWAT during the HRU definition phase. Initially, we
247 isolated loblolly pine and slash pine species from NFTD and saved them as a separate raster layer.
248 Next, the original NLCD 2016 raster layer was overlaid with the NFTD raster. Using the erase

function from the Analysis Tool toolbox and ingesting the NFTD loblolly and slash pine layers as input (one after the other), the NLCD land use classes overlapping with loblolly and slash pine layers were erased. The geospatial information of the previously isolated loblolly and slash pine rasters were then copied (copy function on ArcMap's main toolbar enabled through an edit session) and pasted (paste function on ArcMap's main toolbar) into the NLCD rasters that had their original classes erased in the previous step. It is worth mentioning that this sequential pre-processing was applied to the NLCD's land use classes representing forests only (e.g., forests deciduous, forests evergreen, forests mixed, and forested wetlands), exempting other land use classes such as agricultural lands and urban spaces. This decision was made to avoid misclassification, given the coarser resolution of NFTD compared to NLCD. Table 2 shows the percentage cover of each land use class with respect to the watershed's area, before and after reclassification.

Table 2. Land use and cover change after reclassification to consider loblolly and slash pine spatial distribution across the watersheds

	Upatoi Creek		Upper Santa Fe	
Land use class	% coverage - NLCD 2016	% coverage - Modified NLCD	% coverage - NLCD 2016	% coverage - Modified NLCD

Open Water	3%	3%	0%	0%
Developed, Open Space	4%	4%	6%	6%
Developed, Low Intensity	2%	2%	1%	1%
Developed, Medium Intensity	1%	1%	0%	0%
Developed, High Intensity	0%	0%	0%	0%
Barren Land	0%	0%	1%	1%
Deciduous Forest	14%	3%	2%	0%
Evergreen Forest	30%	4%	40%	5%
Mixed Forest	15%	3%	0%	0%
Shrub/Scrub	9%	9%	6%	6%
Herbaceuous	5%	5%	5%	5%
Hay/Pasture	4%	4%	13%	12%
Cultivated Crops	4%	4%	0%	1%
Woody Wetlands	8%	2%	25%	6%
Emergent Herbaceuous Wetlands	0%	0%	0%	0%
Slash Pine	_	0%		56%
Loblolly Pine	_	57%		1%

For weather forcings, this study used daily precipitation and minimum/maximum temperature from the PRISM Climate Group (http://www.prism.oregonstate.edu), hourly solar radiation and wind speed data from the North American Land Data Assimilation System (NLDAS) (https://ldas.gsfc.nasa.gov/nldas) aggregated to a daily basis, and hourly relative humidity data from the National Solar Radiation Database (NSRD) (Sengupta et al., 2018), also aggregated to daily time-step. Precipitation, temperature, and relative humidity data at 4 km resolution were extracted using the centroid of each subwatershed as a spatial reference, resulting in twenty-three virtual stations at UCW and twenty-one at SFRW. Solar radiation and wind speed estimates at 12.5 km resolution were extracted to all NLDAS grids overlapping the watershed's boundary, which resonated in eight virtual stations at both UCW and SFRW.

To assess the effects of improved SWAT forest parameterization at the watershed scale, we compared SWAT predicted ET and LAI against MODIS-derived estimates. To accomplish

this, we selected subwatersheds almost entirely covered by loblolly and slash pine and then compared SWAT outputs of LAI and ET from the largest HRU against MODIS estimates. MOD15A2H (Myneni et al., 2015) and MOD16A2 (Running et al., 2017) datasets were used to derive LAI and ET data at 4-days and 8-days intervals, respectively, at 500 meters resolution. MODIS extracted data were geo-referenced and spatially aggregated to the shape of previously delineated polygons representing the located loblolly and slash pine areas using automated routines in the Google Earth Engine platform (Gorelick et al., 2017). The simulated forest biomass was compared to gridded forest biomass data from the U.S. Department of Agriculture (USDA) Forest Service Forest Biomass product, which was developed based on field measurements and statistical models (Blackard et al., 2008). Comparison of simulated and observed forest dynamics using the default and re-parameterized models are shown in section S1 of the supplementary materials (Appendix C).

We set up the initial growing conditions of slash and loblolly pine in the models by deleting all management operations assigned to the management file in ArcSWAT. Next, we assumed that trees were fully developed at the beginning of the simulation period by setting the HRU's land cover status as land cover growing from the beginning of the simulation period. Moreover, some initial physical conditions like the number of heat units (*PHU_PLT*), initial leaf area index (*LAI_INIT*), and initial biomass (*BIO_INIT*) had to be defined to configure the annual growth cycle of trees. For loblolly and slash pine, *PHU_PLT* and *LAI_INIT* were defined based on the field-scale model parameterization presented by Haas et al. (2021b) while *BIO_INIT* was initialized according to USDA's Forest Service forest biomass data for each watershed.

For streamflow calibration and validation, we used daily streamflow data from the U.S. Geological Survey (USGS) gaging stations 02341800 and 02321000 at UCW and SFRW,

305 respectively. The complete dataset used for constructing and calibrating/validating the SWAT
306 models, as well as their sources, are summarized in Table 3. Based on the described data,
307 SWAT2012 (revision 664) through the ArcSWAT interface with a 10%-10%-0% (land-use, soils,
308 slope) threshold generated 23 subbasins and 172 HRU's for UCW, whereas, 21 subbasins and 138
309 HRU's were generated for the SFRW. The models were run from 1995 to 2018, using 3 years
310 (1995-1997) of initialization as model warm-up period.

311

312

313

314

315

316

317

318

319

320

321 Table 3. Description of data and their sources. Model input data refers to datasets utilized to construct the watershed
322 models. Model calibration refers to data utilized to constrain intra-watershed processes and calibrate discharge at the
323 watershed's outlet.

Data	Description	Source

Model input data	Topography	National Elevation Dataset at 10 meters resolution	United States Department of Agriculture (USDA) Geospatial Data Gateway (https://datagateway.nrcs.usda.gov/)
	Land use	2016 NLCD	United States Department of Agriculture (USDA) Geospatial Data Gateway (https://datagateway.nrcs.usda.gov/)
	Soil	Gridded Soil Survey Geographic (gSSURGO)	United States Department of Agriculture (USDA) Geospatial Data Gateway (https://datagateway.nrcs.usda.gov/)
	Climate	Daily precipitation, maximum/minimum temperature, solar radiation, wind speed	PRISM climate group (http://www.prism.oregonstate.edu/),National Land Data Assimilation Systems (NLDAS) phase 2 (https://ldas.gsfc.nasa.gov/nldas/NLDAS2model_download.php), National Solar Radiation Database (https://nsrdb.nrel.gov/)
	Atmospheric deposition	Wet and dry deposition of nitrate and ammonia	National Atmospheric Deposition Program (NADP) (http://nadp.slh.wisc.edu/)
Model calibration	Seasonal LAI	4 days composite dataset at 500 meters pixel resolution	Moderate Resolution Imaging Spectroradiometer (MODIS) (https://lpdaac.usgs.gov/products/mcd15a3hv006/)
	ET	8 days composite dataset at 500 meters pixel resolution	Moderate Resolution Imaging Spectroradiometer (MODIS) (https://lpdaac.usgs.gov/products/mod16a2v006/)
	Biomass	Field-measured annual total trees biomass	Long-term field studies conducted FMRC, FBRC, and PMRC in Georgia, Florida and Alabama, respectively
	Annual LAI	Field-measured annual LAI	Long-term field studies conducted FMRC, FBRC, and PMRC in Georgia, Florida and Alabama, respectively
	Streamflow	Daily discharge from stations USGS 02321000 (FL) and USGS 02341800 (GA)	USGS Water data (https://waterdata.usgs.gov/nwis)

2.4.Experimental design

328 Parameter-rich models such as SWAT can be easily calibrated for streamflow even though key
329 intra-watershed processes such as forest dynamics are simulated poorly. This is because an
330 observed signal (e.g., point-scale streamflow) may be reproduced in such models using thousands
331 of different parameter sets or ranges of parameter combinations. This problem is known as
332 equifinality (Beven and Freer, 2001), where, models can give right answers for wrong reasons.
333 One possible way of minimizing the equifinality problem is by constraining more model variables
334 (e.g., LAI, biomass, ET) through additional observed data. Here we perform four modeling
335 experiments before streamflow calibration in which we progressively constrain more variables
336 with additional data. These experiments can help us isolate the impacts of LAI, biomass, and ET
337 on streamflow prediction and water budget computation without the confounding effect stemming
338 from the calibration of streamflow-related parameters. To measure the benefits and drawbacks of
339 each experiment, we compared simulated baseflow, streamflow, watershed-average ET, and runoff
340 coefficient against observations and remote-sensing derived estimates. Observed baseflow was
341 estimated from observed streamflow using the Web-based Hydrograph Analysis Tool (WHAT)
342 (Lim et al., 2005) using its standard settings for perennial streams with a porous aquifer. The
343 experiments were as follows:

344 1. Default model (M_0): SWAT model was setup and run without altering plant growth-related
345 parameters;
346 2. ET (M_{ET}): this experiment added ET-related parameters (transferred from Haas et al.
347 (2021b)) to the default model (M_0);
348 3. LAI + biomass (M_{LAI+BM}): this experiment incorporated parameters controlling LAI and
349 biomass, which were previously calibrated by Haas et al. (2021b);

4. LAI + biomass + ET ($M_{LAI+BM+ET}$): this experiment included calibrated parameter values representing the full coupling of vegetation, water, and energy relations in SWAT.

Comparison of M_{ET}, M_{LAI+BM}, and $M_{LAI+BM+ET}$ against M_0 tells us how much model performance has improved or deteriorated due to the addition/removal of new variables. The fourth experiment ($M_{LAI+BM+ET}$) was the one we were most interested in because it fully considered the tree growth cycle in SWAT and included the largest number of variable constraints. M_{LAI+BM} compared to M_0 tells us how much model performance has improved or deteriorated by including improved phenological development and biomass accumulation without adjusting for canopy evaporation, plant water uptake, and soil evaporation. M_{ET} shows how remote-sensed ET data can help predictions in ungauged basins or watersheds with limited streamflow records. M_0 is a baseline scenario serving as a reference to measure the advantages and disadvantages of M_{ET}, M_{LAI+BM}, and $M_{LAI+BM+ET}$.

2.5. Streamflow calibration and validation strategies

Hydrological models often cannot accurately simulate streamflow under default parameterization. Each watershed is unique and dominant hydrological processes can vary, which default parameterization may not capture. Thus, model calibration is frequently performed to adjust selected model parameters representing the processes of interest. In this study, we employ an automated model calibration approach to enhance SWAT's accuracy in simulating streamflow at the watershed's outlet. We split the time series data into calibration (1998-2014) and validation (2015-2018) periods in both watersheds. SWAT Calibration and Uncertainty Program (SWAT-CUP) (Abbaspour, 2015a), a standalone calibration software developed specifically to be used with SWAT, was used to optimize model parameters. Model calibration was carried out at the daily time step using the Sequential Uncertainty Fitting algorithm (SUFI-2) option in SWAT-CUP.

In SUFI-2, global sensitivity analysis is performed by calculating the regression coefficients of the parameters generated by the Latin hypercube sampling method against the values of the defined objective function. The relative significance of each sampled parameter is measured using a t-test. Parameter sensitivities are computed by quantifying the average changes in the objective function resulting from changes in each parameter (Abbaspour, 2015b). The *p-value* tests the null hypothesis that the coefficient of a parameter is equal to zero (i.e., the parameter is not sensitive). Low *p-values* (typically <0.05) indicate sensitive parameters.

In SUFI-2, uncertainty in parameters is expressed as ranges representing uncertainties associated with forcing input data (e.g., precipitation), the conceptual model, parameters, and observations (Abbaspour, 2015b). Uncertainties in parameters are reflected as uncertainties in the model output variable, which are represented as the 95% probability distributions (95PPU). The 95PPU is hence the model solution in a stochastic calibration approach, considering all sources of uncertainties. SWAT-CUP provides two statistics to quantify the fit between the 95PPU and observed data*: P-factor* and *R-factor*. The *P-factor* expresses the percentage of observed data enveloped by the 95PPU, while the *R-factor* is the relative thickness of the 95PPU band and is calculated as the average of the 95PPU thickness divided by the standard deviation of the corresponding observed variable (Abbaspour et al., 2018). Ideally, most of the observations should be captured by the 95PPU (i.e., *P-factor* close to 1) in a small envelope (i.e., small *R-factor* value).

As model performance measures, this study used the coefficient of determination (R^2), the Nash-Sutcliff-Efficiency (*NSE*), and the percentage bias (*PBIAS*). Further, *NSE* was selected as the objective function in SUFI-2, and 500 simulations were performed per iteration. The number of iterations was based on how fast the model was converging to a higher *NSE* value in the subsequent iteration. The parameters used to calibrate SWAT for streamflow in this study were

396 selected based on the model's structure and equations regulating discharge computation described
397 in Neitsch et al. (2011).

398 We calibrated daily streamflow for the two extreme modeling experiments, namely M_0
399 (default) and $M_{LAI+BM+ET}$ (LAI + biomass + ET). Comparing these two calibration schemes can
400 show the benefits of including all variables describing forest dynamics simulation in model
401 calibration and how it changes the solution space (i.e., the most optimal value within the range of
402 parameters) relative to a model constraint with gauged streamflow data only. Since $M_{LAI+BM+ET}$
403 considers improved LAI, biomass, and ET estimates and theoretically represents the most optimal
404 model condition among the four experiments (i.e., a model able to predict forest attributes and
405 streamflow reasonably well), this experiment was selected to quantify the effects of improved
406 forest processes on automated streamflow calibration. Both calibration approaches are explained
407 below.

408 2.5.1. Traditional model calibration (M_0)

409 Calibration of M_0 involved adjusting the parameters listed in Table S1 for the default model setup.
410 This is a traditional calibration approach employed in most hydrologic modeling studies, where
411 model parameters related to vertical fluxes (e.g., ET) and horizontal fluxes (e.g., surface runoff)
412 are lumped together and calibrated with streamflow data only. This is considered a "simple
413 strategy" (Daggupati et al., 2015), where a single model output variable (e.g., streamflow) is
414 optimized at a single site, such as the watershed outlet. In their guidelines for calibration/validation
415 of hydrologic models, Daggupati et al. (2015) only recommends this strategy for watersheds
416 having uniform characteristics (e.g., climate, land-use, soil, slope). A major drawback of such
417 calibration approach is that it may produce pseudo-accurate models showing statically good
418 performances for streamflow at the watershed's outlet, whilst completely misrepresenting internal

419 watershed processes. This calibration scheme was performed to generate a base condition to which
420 the next calibration configuration could be compared.

421 #### 2.5.2. Multi-facet model calibration ($M_{LAI+BM+ET}$)

422 In this calibration scheme, we decoupled horizontal (streamflow) and vertical (ET) water fluxes
423 by constraining parameter values representing biophysical processes within a physically
424 meaningful range. This approach does not optimize parameters controlling vertical fluxes (e.g.,
425 *CANMX*, *EPCO*, *ESCO*) when performing automated streamflow calibration, which is typically
426 the case in traditional calibration. Such parameters had their values derived for loblolly and slash
427 pine trees at the field-scale level in a previous study by Haas et al. (2021b). At the UCW,
428 previously calibrated parameters controlling the LAI development curve, water loss through ET,
429 and tree total biomass for loblolly pine and slash pine were transferred from the Loblolly 2 – GA
430 and Slash - FL sites described in Haas et al. (2021b). For the SFRW model, loblolly and slash pine
431 calibrated parameters were transferred from pine plantation fields located approximately 25 km
432 south of the watershed outlet, namely Loblolly 3 - FL and Slash – FL in Haas et al. (2021b). The
433 transferred parameter values were extended to HRU's covered by loblolly and slash pine at both
434 watersheds. One could argue that transferring parameter values from field-scale to watershed-scale
435 without further calibration is not adequate because of varying physical conditions (e.g., soil types,
436 weather). Unlike reach/subbasin level parameters in SWAT, plant-specific parameters cannot vary
437 spatially in the plant database. In other words, these parameters are species-specific and even
438 though a given type of plant can be present in several HRU's, its parameter values cannot change
439 from HRU to HRU. This model limitation challenges a spatially distributed calibration of
440 biophysical parameters in SWAT-CUP. Such an effort would essentially result in a lumped
441 calibration inconsistent with the spatially distributed characteristic of remote-sensing data. Thus,

our approach is adequate to capture the importance of forest dynamics in hydrological models since the biophysical parameter values included in $M_{LAI+BM+ET}$ were developed based on species-specific high-quality datasets.

2.6. Ecohydrological flow parameters

To better understand the degree of hydrologic alteration attributable to improved forest parameterization in hydrologic models, we utilized the Indicators of Hydrologic Alterations (IHA) desktop model (TNC 2009). IHA was developed by The Nature Conservancy (TNC) based on Richter et al. (1996) for calculating the characteristics of natural and altered hydrologic regimes. This tool summarizes long periods of daily flow data into 67 statistical parameters representing ecologically relevant conditions. These 67 statistical parameters are subdivided into two groups: the IHA parameters (33 parameters) and the Environmental Flow Component (EFC) parameters (34 parameters). In the current study, we selected 10 IHA parameters and 12 EFC parameters to investigate how an improved representation of forest dynamics processes in SWAT affects model predictions of ecologically relevant flow metrics at the SFRW and UCW from 1998 to 2018. To accomplish this, we fed the IHA desktop model with SWAT-simulated daily time-series of streamflow from the calibrated M_0 and $M_{LAI+BM+ET}$ models as well as with observed time-series of streamflow collected at the outlet of both watersheds (i.e., USGS stations 02341800 and 02321000). Next, we compared the percent deviations in IHA metrics between simulations and observations. The percent error of a given ecohydrological flow metric in relation to the observations was calculated using Eq. 2:

$$dQV_{LULC}=\frac{X_{M0}-X_{LAI+BM+ET}}{X_{LAI+BM+ET}}x\ 100(\%) \quad (2)$$

where, X corresponds to a given ERF metric.

The description and importance of the IHA and EFC parameters used in this study are shown in Table S1 of the supplementary materials (Appendix B). Figure 2 illustrates the methodology employed in the current study.

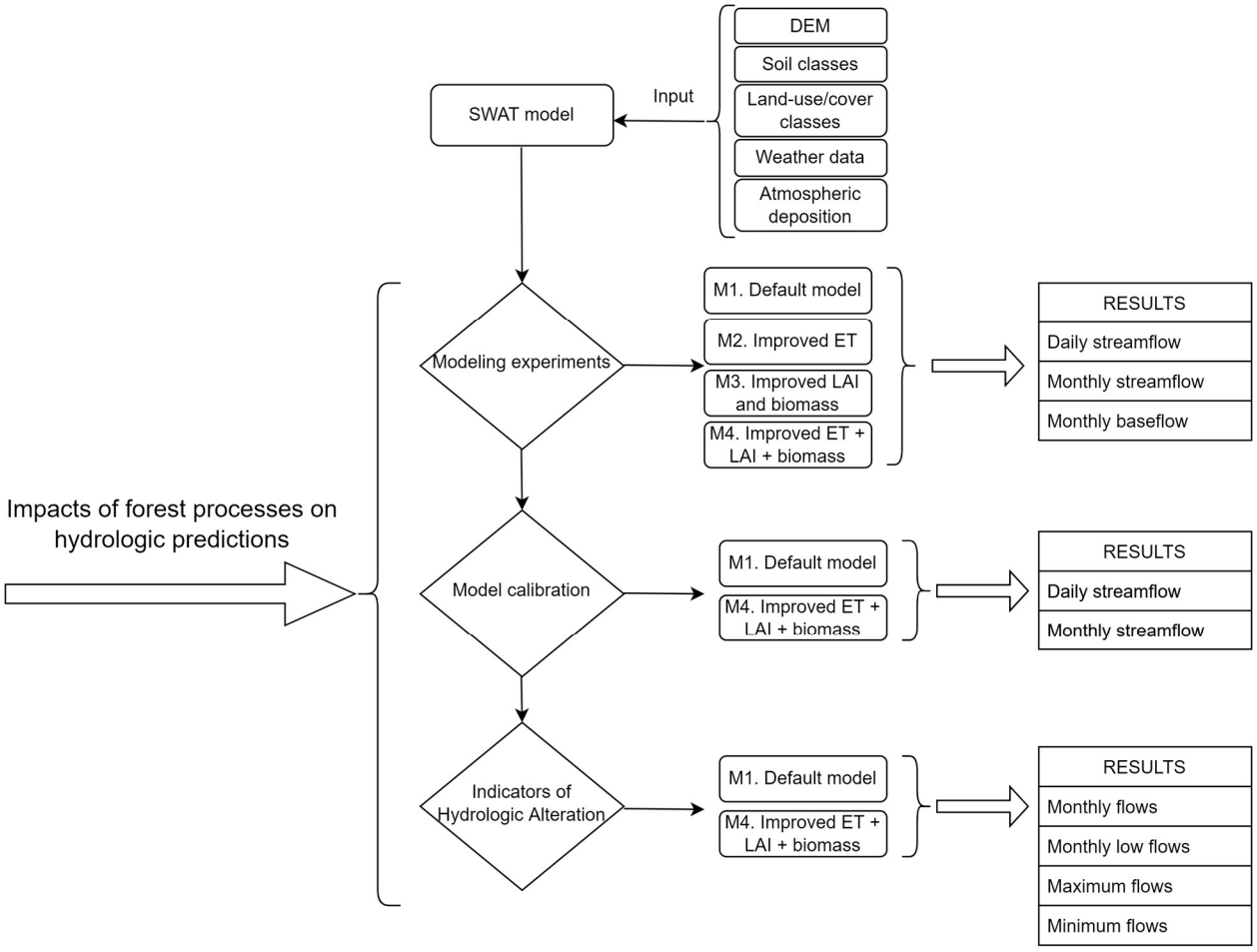

Figure 2. Methodology flowchart.

3. RESULTS AND DISCUSSION

3.1. Hydrological responses to improved forest dynamics

473 The inclusion of improved forest dynamic processes in the model remarkably influenced the
474 watershed hydrological responses. The improvements and drawbacks brought about by each
475 modeling experiment are individually described and discussed below.

476 3.1.1. The baseline model

477 Prior to streamflow calibration, the baseline model configuration M_0 showed poor performance in
478 simulating daily and monthly streamflow, as well as monthly baseflow, at both watersheds (Fig.
479 3-4). Flow duration curves of daily streamflows are shown for both watersheds in Fig. 3. As can
480 be seen, high flows were captured reasonably well in M_0, however, low flows were poorly
481 simulated, especially at SFRW. Overall, daily streamflow was overestimated by 67% and 267% at
482 UCW and SFRW, respectively, and *NSE* values were lower than 0.2 (Fig. 3). Similarly, monthly
483 streamflow showed low *NSE* values and poor agreement with observed data at both watersheds
484 (Fig. 4). M_0 overestimated most of the peaks at both study sites. The monthly baseflow simulated
485 by the SWAT models in M_0 show big differences compared to observations (Fig. 5). M_0
486 overestimated baseflow by 55% at UCW and 460% at SFRW in the period 1998-2018. Simulated
487 mean annual baseflow was also highly overestimated at both study sites compared to the observed
488 data (Fig. S3 of the supplementary materials under Appendix A). The watershed-average ET
489 simulated from 1998 to 2018 at the UCW was 614 mm/year in M_0 (Fig. S2 – of the supplementary
490 materials under Appendix A), 25% lower than MODIS estimates (815 mm/year). Similarly, at the
491 SFRW, the simulated watershed-average ET was 546 mm/year, 57% lower than the MODIS
492 estimated value of 1013 mm/year. Considering MODIS ET data, 24% of rainfall became runoff at
493 SFRW and 37% at UCW. The predicted fractions in M_0 were 59% at SFRW and 52% at UCW,
494 which is the direct consequence of ET underestimation.

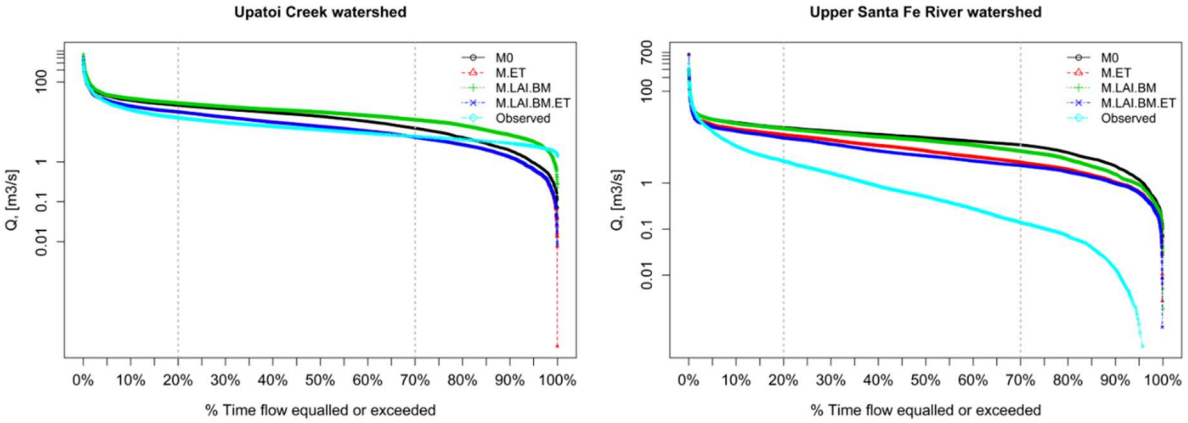

	Upatoi Creek				Upper Santa Fe			
	M_0	M_{ET}	M_{LAI+BM}	$M_{LAI+BM+ET}$	M_0	M_{ET}	M_{LAI+BM}	$M_{LAI+BM+ET}$
NSE	0.19	0.64	-0.13	0.63	-0.36	0.15	-0.23	0.24
PBIAS (%)	-66	-12	-101	-14	-268	-134	-233	-104
R^2	0.62	0.69	0.6	0.68	0.41	0.44	0.42	0.45

Figure 3. Model verification under different configuration setups against USGS observed daily streamflow data for different exceedance probability of simulated streamflow at the watershed outlet from 1999 to 2019 at Upatoi Creek at Upper Santa Fe watersheds. The flow duration curve displayed here is plotted in log scale. The statistical rating metrics displayed in the table refer to daily streamflow variability (not shown), and not to the exceedance probability curves.

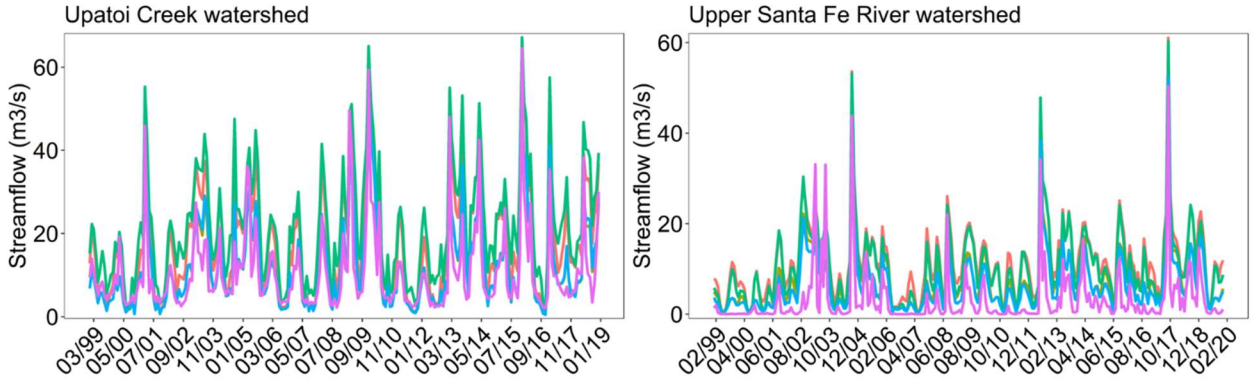

	Upatoi Creek				Upper Santa Fe			
	M_0	M_{ET}	M_{LAI+BM}	$M_{LAI+BM+ET}$	M_0	M_{ET}	M_{LAI+BM}	$M_{LAI+BM+ET}$
NSE	0.03	0.77	-0.71	0.75	-1.35	0.16	-0.93	0.39
PBIAS (%)	-66	-12	-101	-14	-268	-134	-233	-104
R^2	0.77	0.80	0.72	0.79	0.60	0.65	0.61	0.68

Figure 4. Hydrograph showing monthly simulated streamflow against USGS observed data for different model configurations setups from 1999-2019.

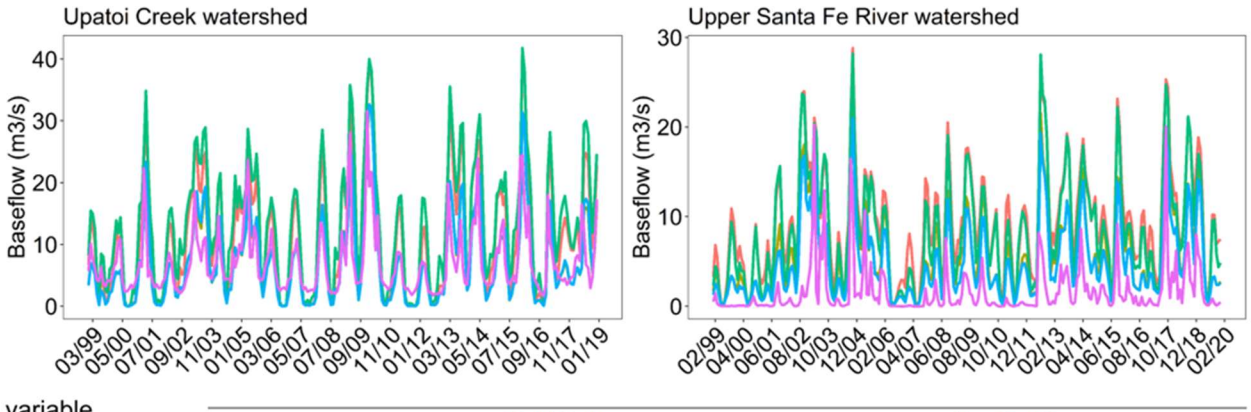

	Upatoi Creek				Upper Santa Fe			
	M_0	M_{ET}	M_{LAI+BM}	$M_{LAI+BM+ET}$	M_0	M_{ET}	M_{LAI+BM}	$M_{LAI+BM+ET}$
NSE	-0.79	0.46	-1.83	0.42	-8.26	-2.32	-6.74	-1.366
PBIAS (%)	-55	0.65	-85	-1.27	-460.7	-245.28	-403.98	-198.4
R2	0.65	0.67	0.6	0.66	0.4	0.46	0.41	0.481

Figure 5. Hydrograph showing monthly simulated baseflow against estimated baseflow for different model configurations setups from 1999-2019. Observed baseflow is estimated via baseflow separation program.

3.1.2. Effect of ET on streamflow simulation

The inclusion of previously calibrated ET parameters in M_{ET} dramatically improved the model's performance for streamflow and baseflow, as evidenced by increased *NSE* values (Fig. 3-4). The consistent model overestimations of streamflow and baseflow produced under M_0 were remarkably decreased at both study watersheds in M_{ET}. The enhanced model performance was particularly alluring at UCW where simulated daily streamflow was overestimated by 12% and baseflow by less than 1%. By analyzing the exceedance probability curves (Fig. 3), it is possible to notice that M_{ET} increased the agreement between simulated and observed streamflow, especially for low flows (≥ 70%) at SFRW. Similarly, monthly peak streamflow and baseflow estimates improved in M_{ET} in comparison to M_0 (Fig. 4 and Fig. 5). The main effect of M_{ET} configuration on the watershed water budget was concerning baseflow (Fig. 6). Increases in annual average ET of 25% at UCW (2% overestimation) and 33% at SFRW (20% underestimation) in M_{ET} compared to M_0 led to reductions in mean annual baseflow of 41% and 40%, respectively. Higher ET simulated in M_{ET} reduced water yields in the watersheds. Under the M_{ET} model configuration, 37% of precipitation

became discharge at UCW, which perfectly matched the 37% calculated using MODIS-derived data. Also, 38% of the incoming precipitation resulted in modeled discharge at the SFRW, relatively close to the 24% estimated using observed data. These findings should not come as a surprise considering that ET is the main component of the forest water budget, having underlying effects on watershed-scale water quantity. Also, studies such as Zhang et al. (2012), Brauman et al. (2012), and Sun et al. (2011) have demonstrated that taller vegetation, such as forest stands, are associated with higher ET rates and consequent lower water yield. Other studies have shown the benefits of constraining ET in hydrological models based on remote-sensing data (Herman et al., 2018; Odusanya et al., 2019; Rajib et al., 2016, 2018; Strauch and Volk, 2013). Our results are in line with studies such as Rajib et al. (2018b), who demonstrated the perks of ingesting remotely-sensed PET from MODIS in simulating streamflow with SWAT. The authors showed that by improving ET estimations, the model predictions of streamflow improved as well, especially concerning high flows. Parajuli et al. (2018) derived time-series of ET from MODIS to enhance SWAT ET predictions and evaluated the impacts on streamflow simulation. Results showed that the model performance in predicting streamflow jumped from a *NSE* value of 0.39 under the default model settings to a value 0.71when considering ET data. In a similar study, Tobin and Bennett (2017) used ET data from the Global Land Evapotranspiration: the Amsterdam Model (GLEAM) to constrain SWAT parameter values related to ET in an experimental watershed in Oklahoma-USA. Their findings indicate a better match between simulated and observed streamflow when considering ET data. In the current study, results of M_{ET} suggest that readily available remote-sensing ET data can help to improve the performance of hydrological models in predicting streamflow and baseflow in ungauged watersheds. This finding concurs well with the study of Y. Zhang et al. (2020), who demonstrated the potential of solely using ET data to calibrate

hydrologic models in 222 ungauged watersheds in Australia. It is worth highlighting that ET-related parameters were not re-calibrated for our study watersheds but rather transferred from the field-scale level. This may indicate that the model performance could be further improved by carrying out a site-specific calibration at each watershed.

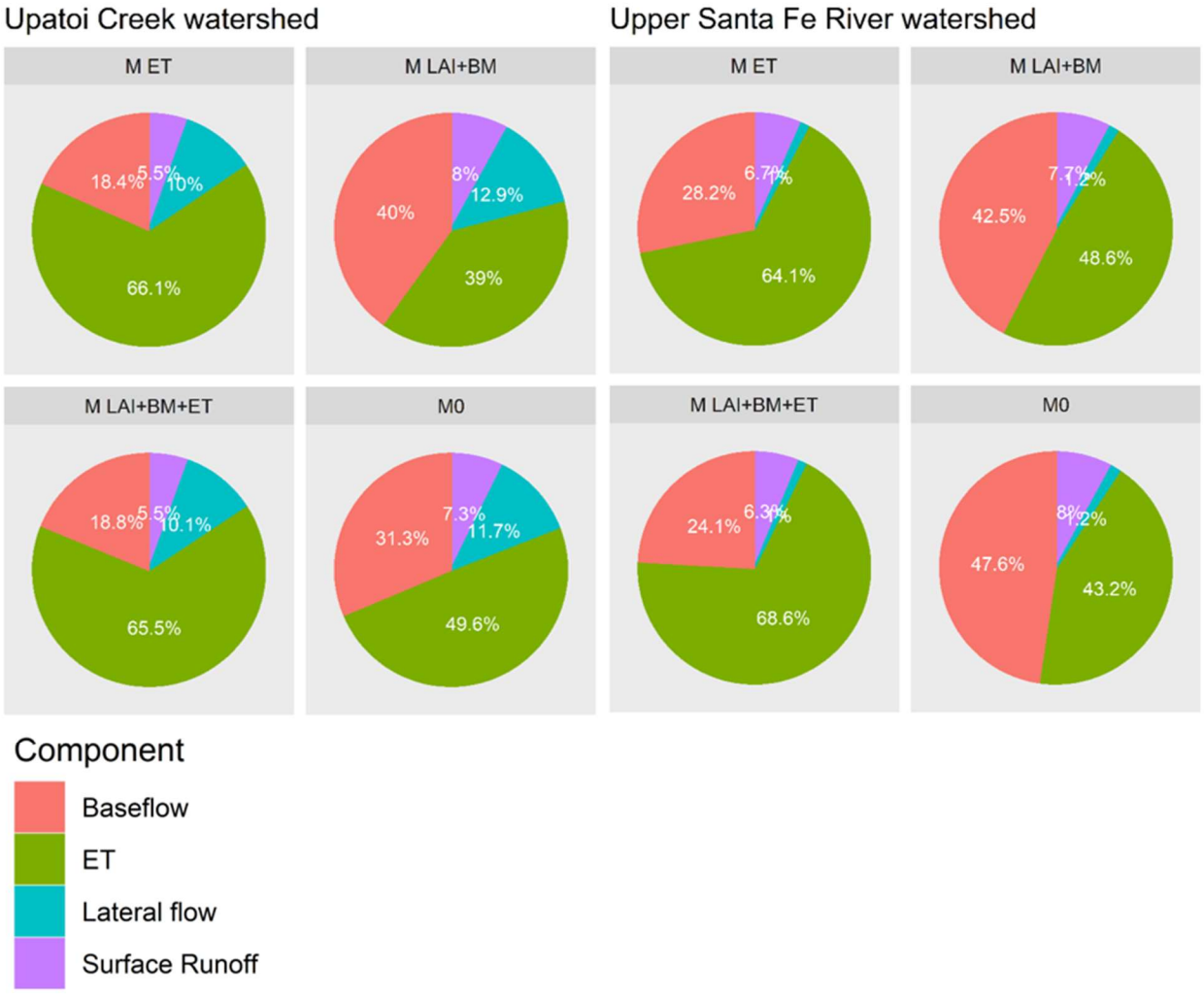

Figure 6. Change in simulated water budget under different model setup configurations from 1999 to 2019 at Upatoi Creek and Upper Santa Fe watersheds.

3.1.3. Effect of LAI and biomass on streamflow simulation

In the next model configuration (M_{LAI+BM}), we added calibrated parameter values regulating LAI and biomass prediction to the baseline model (but removed ET). As shown by the rating metrics and the flow temporal variability displayed in Figures 2-4, the model performance for streamflow and baseflow in M_{LAI+BM} deteriorated compared to M_{ET}. SWAT performed particularly poorly in M_{LAI+BM} at the UCW, where the performance metrics worsened even in comparison to the baseline model M_0. In contrast, M_{LAI+BM} showed superior performance compared to M_0 for all statistical measures at SFRW. This difference can be understood by considering the different tree growth and dynamics of loblolly pine and slash pine. As described in section 2.1, UCW is dominated by loblolly pine while the SFRW is mainly covered by slash pine trees. As shown in Fig. S1 of the supplementary materials (Appendix A), the M_0 configuration considerably overestimated LAI for loblolly pine at UCW, whereas, underestimated it for slash pine at the SFRW. As a result of lower simulated LAI at UCW, after incorporating previously calibrated LAI parameters, compared to M_0, simulated ET in M_{LAI+BM} had decreased 22% (Fig. S3 – of the supplementary materials under Appendix A). Consequently, the simulated baseflow increased 16% in relation to M_0 and was further overestimated (Fig. S3 – of the supplementary materials under Appendix A), which led to the deterioration of model performance under M_{LAI+BM}. As expected, due to lower ET losses in M_{LAI+BM}, the runoff coefficient increased to 0.63, deviating significantly from 0.37 calculated with the observed data. These results are in good accordance with Sun et al. (2011), who highlights that monthly LAI is the single most important biophysical variable regulating ET. At the SFRW, because of larger LAI values obtained after the incorporation of pre-calibrated LAI parameters (Fig. S1 - of the supplementary materials under Appendix A), the M_{LAI+BM} configuration predicted higher ET rates compared to M_0, increasing the watershed-average ET by 12%. Accordingly, the simulated streamflow and baseflow were reduced in M_{LAI+BM} (Fig. S3 - of the supplementary

materials under Appendix A), which ameliorated the model's performance compared to M_0. Besides LAI, the higher stand biomass predicted under M_{LAI+BM} (Fig. S2 - of the supplementary materials under Appendix A) compared to M_0 most likely contributed to the lower water yield and helped mitigating the model overestimation of streamflow observed in the M_0 scenario at the SFRW. This is in good agreement with studies such as McLaughlin et al. (2013), which shows that reduced biomass may lead to reduced ecosystem water use and thus increased regional and local water yield. The extent to which the watershed water balance was impacted by LAI and biomass (Fig. 6) highlights the importance of considering forest dynamics in hydrologic modeling studies, and the necessity of including ET in the modeling spectrum. Past studies have also shown how biophysical variables such as LAI and biomass can help improving streamflow prediction in hydrologic models. For instance, Ma et al. (2019) and Rajib et al. (2020) have replaced SWAT's empirical LAI algorithm with remotely-sensed LAI data assimilated from MODIS. Results showed superior model performances for simulating streamflow and sediment yield in China and United States. Guo et al. (2018) introduced new LAI and biomass algorithms to predict the growth and dynamics of *Populus* trees in SWAT. By constraining LAI and biomass parameters, the authors showed enhanced model performance in predicting streamflow, sediment, and nitrate. Unlike these studies, the methodology tested here does not involve modifying SWAT's source code, but rather improving the representation of forest processes by constraining the model with physically meaningful information derived from remote-sensing, field observations, and published literature. Thus, the improved forest parameterization tested here is readily available and can be broadly useful to the modeling community.

3.1.4. Effect of coupled water, surface land, and energy processes on streamflow simulations

602 Results from $M_{LAI+BM+ET}$ were the most telling in terms of the impacts of forest processes on the
603 model performance of hydrologic predictions. Under $M_{LAI+BM+ET}$, the models were constraint with
604 the largest number of variables among all experiments, and, besides showing the best performance
605 in predicting streamflow and baseflow, the models also predicted forest growth and dynamics
606 reasonably well under this parameterization. At UCW, the model performance for streamflow and
607 baseflow simulations slightly deteriorated compared to M_{ET} but largely improved in relation to M_0
608 and M_{LAI+BM} (Fig. 3-4). Compared to MODIS-derived data, the watershed-average ET predicted
609 in $M_{LAI+BM+ET}$ was less than 1% higher and showed the closest agreement with MODIS estimates
610 among all modeling experiments at the UCW (Fig. S3 - of the supplementary materials under
611 Appendix A). The mean annual baseflow simulated in $M_{LAI+BM+ET}$ also showed good agreement
612 with the observed data (2% overestimation) (Fig. S3 - of the supplementary materials under
613 Appendix A). Although the inclusion of improved LAI and biomass into the model configuration
614 led to the deterioration in model performance compared to M_{ET}, it is more coherent to include
615 biophysical parameters values representing LAI development and biomass accumulation along
616 with ET calibration, given the interplays between tree attributes (e.g., aboveground biomass and
617 canopy) and the volume of water lost to the atmosphere as vapor. Additionally, enhanced model
618 representation of tree attributes such as LAI and biomass may positively influence water quality
619 applications. For instance, the adjusted total biomass to residue ratio *(BIO_LEAF*) from 30% to
620 2% reduces the amount of plant residue on the soil that is available for mineralization and
621 nitrification. Likewise, the sediment yield simulated in SWAT through the Universal Soil Loss
622 Equation (USLE) (Williams, 1975) is affected by the amount of residue on the soil surface. The
623 combined positive effects of M_{ET} and M_{LAI+BM} at SFRW yielded $M_{LAI+BM+ET}$ as the best model
624 configuration at this study site. The agreement between the simulated and observed streamflow

and baseflow at the watershed outlet increased under $M_{LAI+BM+ET}$ (Fig.2-4) compared to the other experimental conditions, as indicated by the highest goodness-of-fit measured by *NSE* and R^2. The model overestimation of horizontal fluxes was also the smallest under $M_{LAI+BM+ET}$ at SFRW. This was mainly because of the better agreement between watershed-average simulated ET and MODIS-derived data (Fig. S3 - of the supplementary materials under Appendix A), which decreased the simulated water yield compared to the other modeling experiments. The runoff coefficient estimated based on simulated ET (0.34) was the closest to the observed runoff coefficient (0.24) among all scenarios. The changes produced in the water balance components, as we progressively moved from one experiment to the next, are shown in Fig. 6. There was a significant difference between M_0 and $M_{LAI+BM+ET}$, with a drastic increase in predicted ET and consequent decrease in predicted baseflow under the $M_{LAI+BM+ET}$ configuration at both watersheds. The water balance of $M_{LAI+BM+ET}$ at both watersheds concurs with the findings of Amatya and Skaggs (2011) and Amatya et al. (1996), which indicate that streamflow is mainly derived from subsurface flow (i.e., lateral flow and baseflow) in forested ecosystems, where surface runoff is usually low. The results of $M_{LAI+BM+ET}$ indicate that the main improvement in streamflow and baseflow prediction came from the ET component. Studies such as Strauch and Volk (2013) and Alemayehu et al. (2017) also reported improvements in modeled streamflow under enhanced LAI and ET predictions. Similarly, Yang et al. (2018) showed how enhanced biomass and ET estimates can improve the model's performance in simulating streamflow and sediment losses in a forested watershed. Our findings are also in line with Rajib et al. (2018) and Ha et al. (2018), who showed the benefits of incorporating improved biophysical parameters values regulating variables such as LAI and ET for predicting streamflow with SWAT. However, our study is the first to fully consider

647 the effects of forest dynamics (i.e., LAI, biomass, and ET) on hydrological processes by
648 constraining parameter values representing nationally relevant tree species.

649 ### 3.2. Impact of forest dynamics on streamflow calibration and validation

650 As mentioned earlier, SWAT was calibrated for streamflow only under M_0 and $M_{LAI+BM+ET}$. Note
651 again that M_0 represents the current practice in watershed modeling. Based on the visual
652 comparison and statistical measures, $M_{LAI+BM+ET}$ proved to be a better model in predicting daily
653 streamflow at both watersheds during the calibration and validation periods (Fig. 7). According to
654 the model performance evaluation criteria proposed by Moriasi et al. (2015), the results achieved
655 with the multi-facet calibration scheme ranged from "good" to "very good" at UCW, and
656 "satisfactory" to "very good" at SFRW. Under the traditional calibration scheme, the model
657 performance fell within the same range of categories at UCW but deteriorated to unsatisfactory-
658 satisfactory at SFRW.

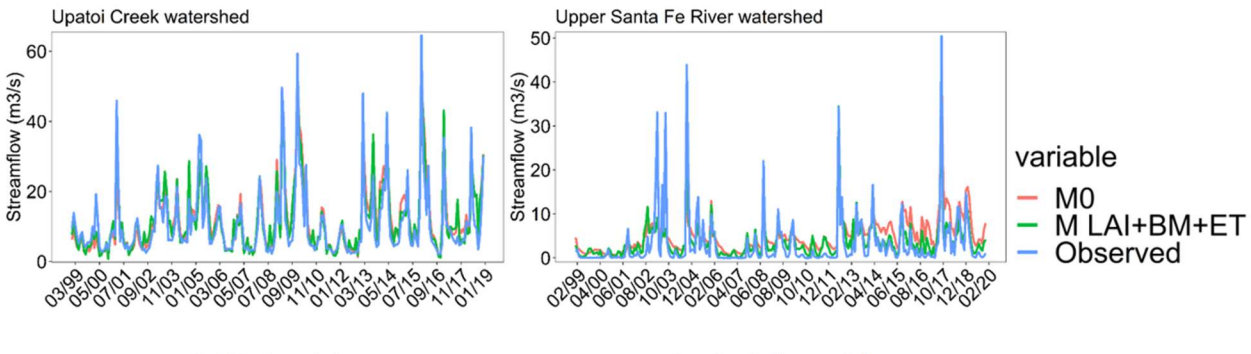

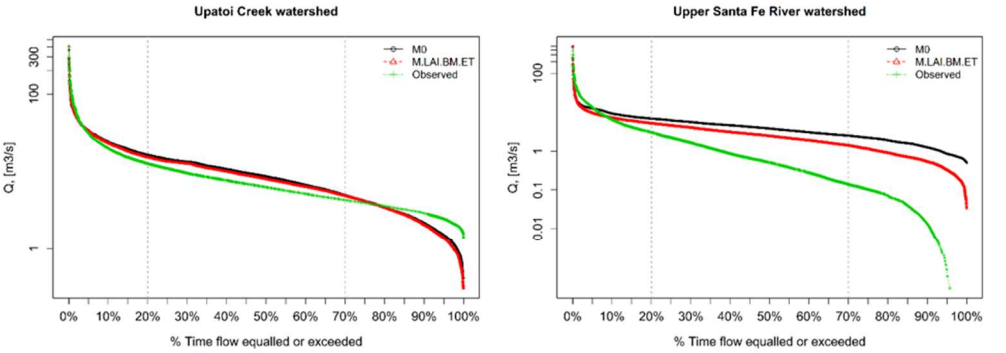

	Upatoi Creek				Upper Santa Fe			
	Calibration (1999-2014)		Validation (2015-2019)		Calibration (1999-2014)		Validation (2015-2019)	
	M_0	$M_{LAI+BM+ET}$	M_0	$M_{LAI+BM+ET}$	M_0	$M_{LAI+BM+ET}$	M_0	$M_{LAI+BM+ET}$
NSE	0.72	0.76	0.78	0.8	0.41	0.52	0.57	0.73
PBIAS (%)	-10.15	-8.09	-22.04	-14.27	-42.9	-19.34	-113.5	-23.9
R2	0.73	0.76	0.79	0.8	0.42	0.52	0.68	0.74

Figure 7. Observed vs. simulated daily streamflow in calibration and validation periods under traditional and multi-facet calibration approaches. The upper hydrographs show the monthly discharge evolution in the period 1999-2019, while the bottom flow duration curves show exceedance probability of simulated streamflow at the watershed outlet from 1999 to 2019 at Upatoi Creek at Upper Santa Fe watersheds. The flow duration curve displayed here is plotted in log scale. The statistical rating metrics displayed in the table refer to daily streamflow variability.

The enhanced model performance achieved with the multi-facet calibration scheme shows that better representation of forest dynamic processes enables SWAT to yield more accurate streamflow estimates. Our findings are in disagreement with the results of studies such as Herman et al. (2018), Dembélé et al. (2020), and Gui Ziling et al. (2019), which suggest that the improvement of terrestrial processes such as ET and soil moisture resonates in lower model performance in predicting in-stream fluxes at the watershed's outlet. In the aforementioned studies, the authors pursued a spatially-distributed calibration approach of terrestrial variables by constraining ET- and/or soil moisture-related parameters for each subwatershed. A pitfall of such

674 an approach is that it lumps land use/cover classes together and does not consider species-specific
675 characteristics. For instance, it is fair to assume that the ET rates of forests and shrubs are
676 substantially different and that fitting parameter values to satisfy both species according to an
677 objective-function may misrepresent both species and lead to unrealistic parameter values. On the
678 other hand, under our calibration approach, we tune the parameter values to dominant tree species.
679 Our results also highlight the advantages of decoupling horizontal hydrological fluxes (i.e.,
680 streamflow) from vertical hydrological fluxes (i.e., ET) when calibrating watershed models. In the
681 traditional calibration approach, ET-related parameters such as *CANMX*, *EPCO*, and *ESCO* were
682 calibrated simultaneously with parameters regulating the horizontal water flux. Although this led
683 to an increased mean annual ET in M_0, the watershed-average annual ET was still lower compared
684 to MODIS estimates. This underestimation of rainfall lost through ET resulted in a higher
685 overestimation of simulated streamflow in M_0 compared to $M_{LAI+BM+ET}$ (Fig. 7). Moreover, in the
686 calibration period, the obtained values of *P-factor* and *R-factor* were 0.07/0.73 at SFRW/UCW,
687 and 0.19/0.58 at SFRW/UCW, respectively, with the traditional calibration approach. Under the
688 multi-facet calibration scheme, *P-factor* and *R-factor* ranged from 0.09-0.72 and 0.11-0.50,
689 respectively. While the values of *P-factor* did not change much according to the calibration
690 approach employed, *R-factor* showed a considerable decrease with the multi-facet calibration
691 scheme, suggesting reduced uncertainties due to consideration of improved forest dynamic
692 processes in the modeling framework.

693 Results from the global sensitivity analysis revealed that *CN*2 is the most sensitive
694 streamflow parameter at both watersheds under M_0 and $M_{LAI+BM+ET}$ (Fig. S4 – of the
695 supplementary materials under Appendix A). However, the rank of sensitive parameters changed
696 in response to the calibration approach utilized. Parameters such as saturated soil hydraulic

conductivity (*SOL_K*), groundwater revap coefficient (*GW_REVAP*), groundwater delay time (*GW_DELAY*), and deep aquifer percolation factor (*RCHRG_DP*) became less sensitive in the multi-facet calibration scheme at the UCW. An opposite trend was observed at the SFRW, where most of the groundwater-related parameters had their sensitivity increased under the multi-facet model calibration scheme, as indicated by lower *p-values* in Fig. S4 (of the supplementary materials under Appendix A). This may be related to the higher baseflow:precipitation ratio observed in the SFRW compared to the UCW (Fig. 6).

A similar effect can be noticed by paying closer attention to the best parameter values found with the traditional and multi-facet calibration schemes (Table S3 - of the supplementary materials under Appendix B). Parameters such as *RCHRG_DP* and *GW_DELAY*, for instance, witnessed substantial changes in their best-fitted values depending on the calibration approach. At both study sites, *RCHRG_DP* decreased in the multi-facet calibration scheme, which is most probably because of higher ET losses in $M_{LAI+BM+ET}$ compared to M_0. In the traditional calibration approach, because of the underestimated ET rates in M_0, the models tended to lose more water through deep aquifer percolation in order to compensate for streamflow overestimation. Similarly, the improved forest dynamics considered in the multi-facet calibration scheme decreased the lag between the time that water exits the soil profile and recharges the shallow aquifer (*GW_DELAY*). Because of excessive water yield and percolation produced in M_0, the traditional calibration scheme slowed down the recharge to the shallow aquifer by assigning larger values to *GW_DELAY*.

Although the traditional calibration approach was able to yield a “very good” model performance in predicting streamflow, it massively failed to accurately replicate key forest dynamic processes such as LAI and biomass within the watersheds (Figures S1 and S2 – of the

720 supplementary materials under Appendix A). This "very good" model performance for streamflow
721 was accomplished at the cost of an excessively high deep aquifer percolation and lumped values
722 of parameters regulating plant transpiration (*EPCO*), soil evaporation (*ESCO*), and canopy storage
723 (*CANMX*) (Table S3 - of the supplementary materials under Appendix B). Alternatively, the multi-
724 facet calibration scheme demonstrated the feasibility of constructing realistic models that can
725 reasonably represent forest processes without losing accuracy in predicting streamflow. Our study
726 is a prime illustration of the concept of equifinality, where models calibrated based on different
727 parameter values may yield equally good outputs (Beven, 2006; Beven and Freer, 2001).
728 Equifinality has been widely associated with semi-distributed watershed models such as SWAT
729 (Ficklin and Barnhart, 2014; Her and Chaubey, 2015; Shen et al., 2012). As highlighted by studies
730 such as Tobin and Bennett (2017), equifinality can be mitigated by constraining the model with
731 more observations. This is demonstrated here, where models constrained by intra-watershed
732 processes such as LAI, ET, and biomass showed improved performance and reduced uncertainties
733 in predicting streamflow, giving the right answers for the right reasons. Although forest dynamics
734 are usually overlooked in watershed modeling studies, we highlight the study of Fernandez-
735 Palomino et al. (2020), which also showed how the calibration of species-specific LAI and ET can
736 improve the simulation of streamflow in SWAT. It is time for watershed modelers to incorporate
737 spatially-distributed information such as remote-sensing based time-series into the modeling
738 framework in order to build models that accurately capture terrestrial and aquatic processes. That
739 said, we believe that our study may open new avenues and bring contributions towards more
740 realistic applications of watershed models.

741 3.3. Impact of forests on ecological flows

742 Biotic processes such as vegetation growth may affect the hydrologic regime within the watershed
743 (Caro Camargo and Velandia Tarazona, 2019; Dalzell and Mulla, 2018; McLaughlin et al., 2013;
744 Mwangi et al., 2016). However, the interplays between the forest and hydrological processes and
745 their watershed-scale effects may not be immediately evident based only on simplistic analysis
746 such as daily and seasonal streamflow, baseflow hydrographs, and mean annual water balance.

747 Figure 8 illustrates the effect of improved forest processes on the relative error of simulated
748 mean monthly flows at both study watersheds. At the UCW, 9 out of 12 parameters showed a
749 smaller percent deviation in relation to the observations under the $M_{LAI+BM+ET}$ model configuration,
750 where the inclusion of enhanced forest dynamic processes reduced the model overestimation of
751 mean monthly flows (Fig. 8a). The only cases where M_0 outperformed $M_{LAI+BM+ET}$ in simulating
752 mean monthly flows were for March, August, and September. At the SFRW, improved forest
753 dynamics also reduced model overestimation of monthly flows, all of which showed better
754 agreement with observation under $M_{LAI+BM+ET}$ (Fig. 8b). The relatively high percent deviation of
755 simulated monthly flows at the SFRW is most likely related to the higher model overestimation of
756 streamflow and poorer performance compared to the UCRW model (Fig. 7). Since monthly flows
757 represent the normal mean daily water conditions for a given month, accurate predictions can be
758 valuable for water resources management applications. Additionally, the magnitude of monthly
759 flows have impacts on aquatic ecosystems and can influence habitat availability, the availability
760 of water for terrestrial animals, besides affecting physical characteristics such as water temperature
761 and oxygen concentrations (Richter et al., 1996; TNC, 2009).

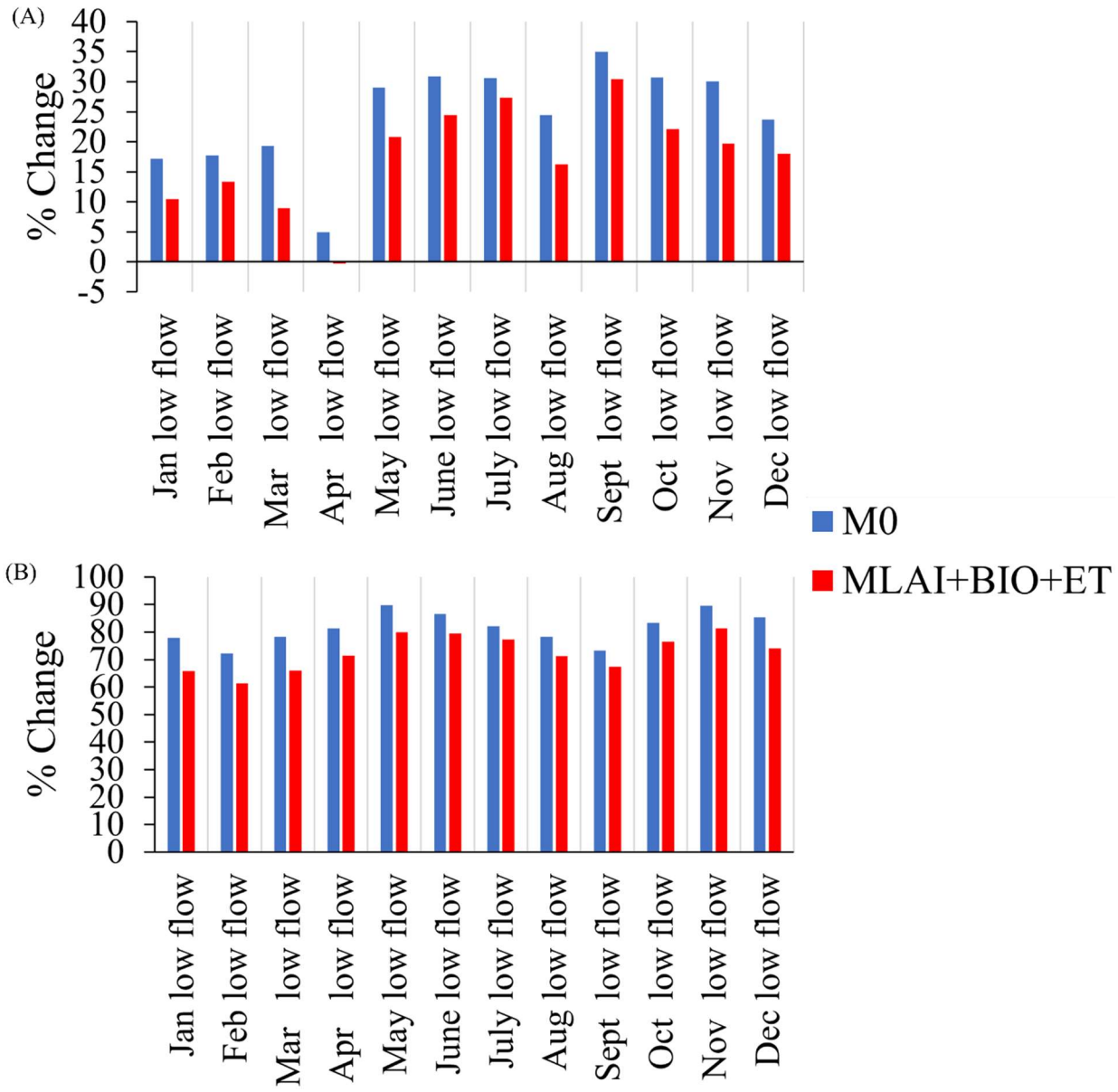

Figure 8. Percentage change of simulated monthly low flow with traditional and multi-facet model calibration in relation to observed USGS daily streamflow data from 1999 to 2019 at Upatoi Creek (A), and Upper Santa Fe River watersheds (B).

The enhanced representation of forest processes in SWAT also resonated in the overall improvement of the model performance for simulating extreme flows of various durations at both watersheds (Fig. 9). At the UCW, $M_{LAI+BM+ET}$ yielded smaller percent errors than M_0 in replicating maximum flows of daily (1-day, 3-days), weekly (7-days), monthly (30 days), and seasonal

771 durations (90-days), besides showing better agreement with observations in predicting minimum
772 flows of monthly and seasonal durations (Fig. 9a). $M_{LAI+BM+ET}$ performed poorer than M_0 in
773 simulating minimum flows of daily and weekly durations. Similar results were found at the SFRW,
774 where model simulations of extreme flows under $M_{LAI+BM+ET}$ returned smaller percent deviations
775 from the observations (Fig. 9b). The only exceptions were maximum flows of daily and seasonal
776 durations for which the model performance deteriorated under $M_{LAI+BM+ET}$ compared to M_0. As
777 shown in Fig. 7, low flows were substantially overestimated at the SFRW, which may help to
778 interpret the large and positive percent deviation of minimum flows found at this watershed.
779 Overall, improved forest dynamics mitigated SWAT's overestimation/underestimation of
780 minimum/maximum flows at the SFRW. These findings are relevant considering the importance
781 of extreme flows for water resources management (Wheater and Evans, 2009), flood control
782 (Archer et al., 2007; Arnaud et al., 2002), infrastructure design (Hailegeorgis and Alfredsen, 2017;
783 Pregnolato et al., 2016), and ecosystems health (Kiesel et al., 2017; Richter et al., 1996), and
784 indicate that the benefits of accurately representing forest processes in watershed models
785 extrapolate improved streamflow simulation.

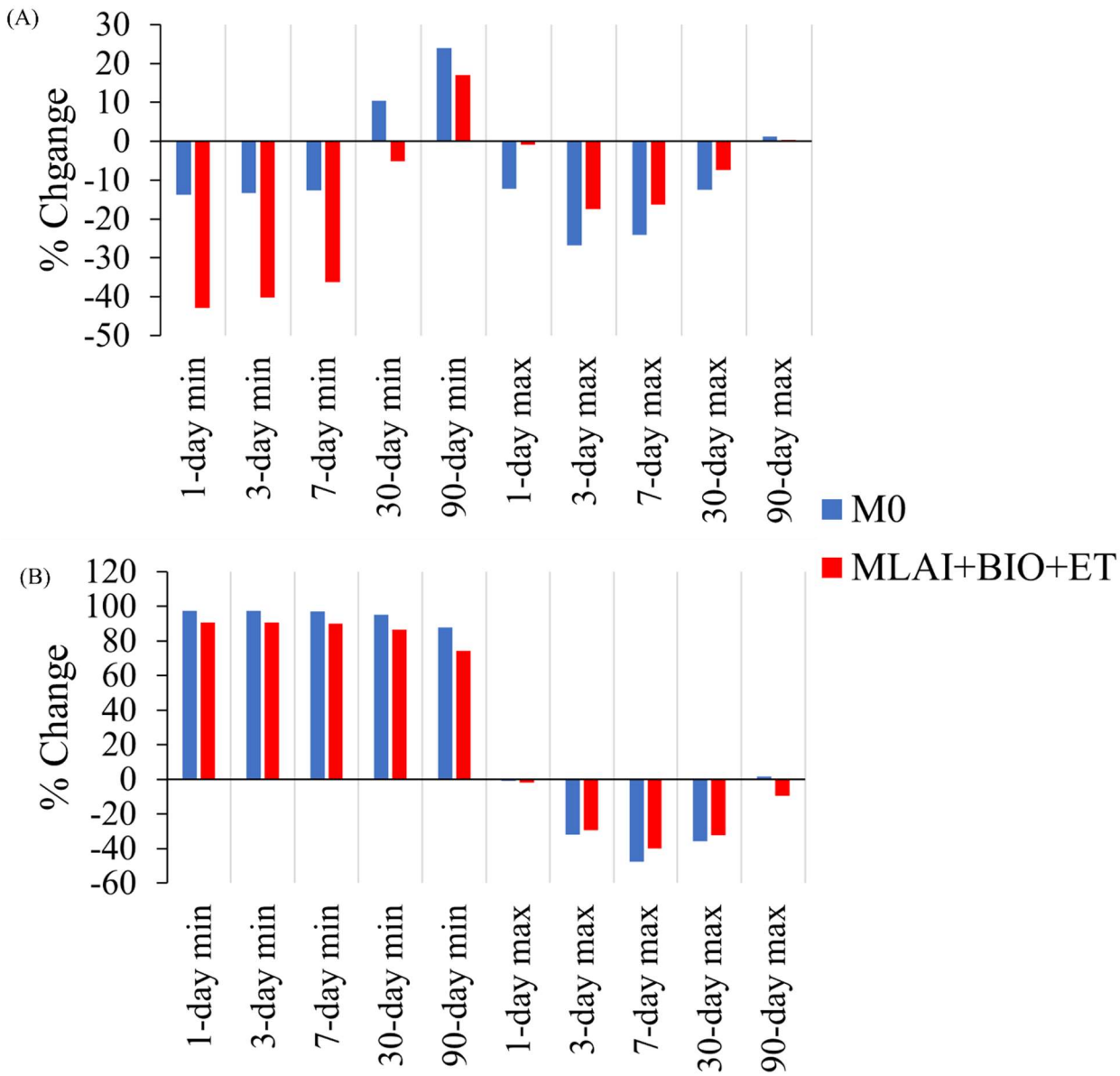

Figure 9. Percentage change of simulated extreme flows with traditional and multi-facet model calibration in relation to observed USGS daily streamflow data from 1999 to 2019 at Upatoi Creek (A), and Upper Santa Fe River watersheds (B).

3.4. Broader implications and limitations

Although our improved forest parameterization relied on field observations from nearby pine plantation fields, we did not have field-measured data within the study watersheds. Thus, our methodological insights were validated against remotely sensed LAI and ET and gridded biomass

795 data. As with any remote-sensing estimate, there are uncertainties associated with MODIS LAI
796 and ET data (Jensen et al., 2011; Long et al., 2014), as well as with the USDA Forest Service forest
797 biomass data. While it may raise uncertainties concerning the validity of our findings, the global
798 coverage of MODIS data facilitates the replication of our methodology worldwide. Moreover,
799 SWAT's flexible plant database allows other researchers to further refine our forest
800 parameterization for other evergreen species.

801 In this study, the focus of our modeling effort was on streamflow and baseflow predictions.
802 The impacts of improved forest growth and dynamics on modeled water quality (e.g., sediment
803 yield, nutrient load) must be addressed in a future endeavor. As demonstrated here, increased ET
804 losses resulting from our improved forest parameterization led to decreased surface runoff and
805 baseflow. It can be inferred that lower surface runoff and baseflow rates will likely decrease
806 sediment and nutrient loads transported to the main channel. Additionally, the adjusted amount of
807 biomass converted to residue every year reduces the source of fresh residue on the soil surface
808 available for mineralization and nitrification. Consequently, the forest parameterization tested in
809 this study may resonate in less nitrate being transported to water bodies. The sediment loss may
810 also be impacted by the improved forest parameterization, especially because the USLE's cover
811 and management factor is computed as a function of plant residue.

812 ## 4. SUMMARY AND CONCLUSIONS

813 The improved representation of forest processes in SWAT returned better streamflow and
814 baseflow predictions. This was demonstrated by performing four modeling experiments aiming to
815 show the individual impacts of LAI, biomass, and ET on water fluxes. Results showed that
816 improved ET prediction is the main reason leading to more accurate streamflow and baseflow

817 simulations in watershed models. The improvements in forest processes substantially altered the
818 watershed water budget towards increased ET and decreased baseflow rates.

819 By calibrating streamflow-related parameters with and without the inclusion of improved
820 LAI, biomass, and ET, we demonstrated that a physically meaningful representation of forest
821 hydrological processes led to superior model performance in predicting streamflow. Moreover, the
822 improved forest parameterization decreased the uncertainties associated with daily streamflow
823 prediction. The importance of forest dynamics was further scrutinized by analyzing multiple
824 ecohydrological parameters. Our results point to the importance of accurately accounting for forest
825 processes in watershed models, especially in highly forested watersheds. The latter not only yields
826 a more realistic model, but also enhances the model's performance in predicting streamflow,
827 reduces the model uncertainties, and improves the terrestrial and aquatic connections, as
828 demonstrated by the 22 ecohydrological parameters considered here.

829 Given the considerable disparity between the two extreme model configurations (i.e., M_0
830 and $M_{LAI+BM+ET}$) in replicating the watershed water budget, the conclusions drawn by each model
831 would largely differ. This could generate impacts on management decisions in case the models
832 were employed to support decision-making. Therefore, we suggest that key forest processes such
833 as LAI, biomass, and ET should be ameliorated in hydrological models before simulating
834 streamflow.

835 Finally, by constraining the models with readily available remote-sensing data we were
836 able to decouple vertical water fluxes and processes (e.g., evapotranspiration, plant water uptake,
837 soil evaporation, and canopy storage) from horizontal water fluxes (i.e., streamflow) in model
838 calibration. This allowed us to simultaneously capture forest dynamics and in-stream processes
839 reasonably well. Such a level of detail and representation of plant-water-energy relations would

hardly be obtained through model calibration against gauged streamflow data only. Considering that the ultimate goal of watershed modeling studies is typically drawing scenario analysis representing different real-world conditions, a model able to accurately represent terrestrial and in-stream processes can produce positive implications for watershed modeling applications.

Acknowledgments

We would like to thank USDA-NIFA (AFRI Water for Agriculture Challenge Area Grant 2017 68007-26319 and 2020-67019-31025) and NOAA-RESTORE Science Program under award NA19NOS4510194 to Auburn University for providing funding for this research.

References

Abbaspour, K.C., 2015a. SWAT Calibration and Uncertainty Programs. Eawag aquatic research. Eawag: Swiss Federal Institute of Aquatic Science and Technology 100.

Abbaspour, K.C., 2015b. SWATCalibration and Uncertainty Programs 100.

Abbaspour, K.C., Vaghefi, S.A., Srinivasan, R., 2018. A Guideline for Successful Calibration and Uncertainty Analysis for Soil and Water Assessment: A Review of Papers from the 2016 International SWAT Conference. Water 10, 6. https://doi.org/10.3390/w10010006

Abou Rafee, S.A., Uvo, C.B., Martins, J.A., Domingues, L.M., Rudke, A.P., Fujita, T., Freitas, E.D., 2019. Large-Scale Hydrological Modelling of the Upper Paraná River Basin. Water 11, 882. https://doi.org/10.3390/w11050882

Adla, S., Tripathi, S., Disse, M., 2019. Can We Calibrate a Daily Time-Step Hydrological Model Using Monthly Time-Step Discharge Data? Water 11, 1750. https://doi.org/10.3390/w11091750

Ahn, S.R., Jeong, J.H., Kim, S.J., 2016. Assessing drought threats to agricultural water supplies under climate change by combining the SWAT and MODSIM models for the Geum River basin, South Korea. Hydrological Sciences Journal/Journal des Sciences Hydrologiques 61, 2740–2753. https://doi.org/10.1080/02626667.2015.1112905

Akhavan, S., Abedi-Koupai, J., Mousavi, S.-F., Afyuni, M., Eslamian, S.-S., Abbaspour, K.C., 2010. Application of SWAT model to investigate nitrate leaching in Hamadan–Bahar Watershed, Iran. Agriculture, Ecosystems & Environment 139, 675–688. https://doi.org/10.1016/j.agee.2010.10.015

Alemayehu, T., Griensven, A. van, Woldegiorgis, B.T., Bauwens, W., 2017. An improved SWAT vegetation growth module and its evaluation for four tropical ecosystems. Hydrology and Earth System Sciences 21, 4449–4467. https://doi.org/10.5194/hess-21-4449-2017

Amatya, D.M., Sun, G., Rossi, C.G., Ssegane, H.S., Nettles, J.E., Panda, S., 2015. Forests, land use change, and water. CRC Press 2015, 116–153.

Amatya, D.M., Skaggs, R.W., 2011. Long-term hydrology and water quality of a drained pine plantation in North Carolina. American Society of Agricultural and Biological Engineers 54, 2087–2098.

875 Amatya, D.M., Skaggs, R.W., Gregory, J.D., 1996. Effects of controlled drainage on the hydrology of
876 drained pine plantations in the North Carolina coastal plain. Journal of Hydrology 1–4, 211–232.
877 Anand, J., Gosain, A. k., Khosa, R., 2018. Prediction of land use changes based on Land Change Modeler
878 and attribution of changes in the water balance of Ganga basin to land use change using the
879 SWAT model. Science of the Total Environment 644, 503–519.
880 https://doi.org/10.1016/j.scitotenv.2018.07.017
881 Anjum, M.N., Ding, Y., Shangguan, D., 2019. Simulation of the projected climate change impacts on the
882 river flow regimes under CMIP5 RCP scenarios in the westerlies dominated belt, northern
883 Pakistan. Atmospheric Research 227, 233–248. https://doi.org/10.1016/j.atmosres.2019.05.017
884 Archer, D.R., Leesch, F., Harwood, K., 2007. Learning from the extreme River Tyne flood in January 2005.
885 Water and Environment Journal 21, 133–141. https://doi.org/10.1111/j.1747-
886 6593.2006.00058.x
887 Arnaud, P., Bouvier, C., Cisneros, L., Dominguez, R., 2002. Influence of rainfall spatial variability on flood
888 prediction. Journal of Hydrology 260, 216–230. https://doi.org/10.1016/S0022-1694(01)00611-4
889 Arnold, J.G., Srinivasan, R., Muttiah, R.S., Williams, J.R., 1998. Large Area Hydrologic Modeling and
890 Assessment Part I: Model Development1. JAWRA Journal of the American Water Resources
891 Association 34, 73–89. https://doi.org/10.1111/j.1752-1688.1998.tb05961.x
892 Awan, U.K., Ismaeel, A., 2014. A new technique to map groundwater recharge in irrigated areas using a
893 SWAT model under changing climate. Journal of Hydrology 519, 1368–1382.
894 https://doi.org/10.1016/j.jhydrol.2014.08.049
895 Beven, K., Freer, J., 2001. Equifinality, data assimilation, and uncertainty estimation in mechanistic
896 modelling of complex environmental systems using the GLUE methodology. Journal of
897 Hydrology 249, 11–29. https://doi.org/10.1016/S0022-1694(01)00421-8
898 Blackard, J.A., Finco, M.V., Helmer, E.H., Holden, G.R., Hoppus, M.L., Jacobs, D.M., Lister, A.J., Moisen,
899 G.G., Nelson, M.D., Riemann, R., Ruefenacht, B., Salajanu, D., Weyermann, D.L., Winterberger,
900 K.C., Brandeis, T.J., Czaplewski, R.L., McRoberts, R.E., Patterson, P.L., Tymcio, R.P., 2008.
901 Mapping U.S. forest biomass using nationwide forest inventory data and moderate resolution
902 information. Remote Sensing of Environment, Remote Sensing Data Assimilation Special Issue
903 112, 1658–1677. https://doi.org/10.1016/j.rse.2007.08.021
904 Brauman, K.A., Daily, G.C., Duarte, T.K., Mooney, H.A., 2007. The Nature and Value of Ecosystem
905 Services: An Overview Highlighting Hydrologic Services. Annual Review of Environment and
906 Resources 32, 67–98. https://doi.org/10.1146/annurev.energy.32.031306.102758
907 Brauman, K.A., Freyberg, D.L., Daily, G.C., 2012. Potential evapotranspiration from forest and pasture in
908 the tropics: A case study in Kona, Hawai'i. Journal of Hydrology 440–441, 52–61.
909 https://doi.org/10.1016/j.jhydrol.2012.03.014
910 Brighenti, T.M., Bonumá, N.B., Grison, F., Mota, A. de A., Kobiyama, M., Chaffe, P.L.B., 2019. Two
911 calibration methods for modeling streamflow and suspended sediment with the swat model.
912 Ecological Engineering 127, 103–113. https://doi.org/10.1016/j.ecoleng.2018.11.007
913 Brown, S.C., Versace, V.L., Lester, R.E., Todd Walter, M., 2015. Assessing the impact of drought and
914 forestry on streamflows in south-eastern Australia using a physically based hydrological model.
915 Environ Earth Sci 74, 6047–6063. https://doi.org/10.1007/s12665-015-4628-8
916 Brown, T.C., Froemke, P., Mahat, W., Ramirez, J.A., 2016. Mean Annual Renewable Water Supply of the
917 Contiguous United States. Briefing paper. Rocky Mountain Research Station, Fort Collins, CO. 55
918 pp.
919 Bruijnzeel, L.A., 2004. Hydrological functions of tropical forests: not seeing the soil for the trees?
920 Agriculture, Ecosystems & Environment, Environmental Services and Land Use Change: Bridging
921 the Gap between Policy and Research in Southeast Asia 104, 185–228.
922 https://doi.org/10.1016/j.agee.2004.01.015

Caro Camargo, C.A., Velandia Tarazona, J.E., 2019. The effect of changes in vegetation cover on the hydrological response of the sub-basin Los Pozos. DYNA 86, 182–191. https://doi.org/10.15446/dyna.v86n208.74115

Chu, T.W., Shirmohammadi, A., Montas, H., Sadeghi, A., 2004. Evaluation of the Swat Model's Sediment and Nutrient Components in the Piedmont Physiographic Region of Maryland. Transactions of the ASAE 47, 1523–1538. https://doi.org/10.13031/2013.17632

Dalzell, B.J., Mulla, D.J., 2018. Perennial vegetation impacts on stream discharge and channel sources of sediment in the Minnesota River Basin. Journal of Soil and Water Conservation 73, 120–132. https://doi.org/10.2489/jswc.73.2.120

Dosdogru, F., Kalin, L., Wang, R., Yen, H., 2020. Potential impacts of land use/cover and climate changes on ecologically relevant flows. Journal of Hydrology 584, 124654. https://doi.org/10.1016/j.jhydrol.2020.124654

Dembélé, M., Hrachowitz, M., Savenije, H.H.G., Mariéthoz, G., Schaefli, B., 2020. Improving the Predictive Skill of a Distributed Hydrological Model by Calibration on Spatial Patterns With Multiple Satellite Data Sets. Water Resources Research 56, e2019WR026085. https://doi.org/10.1029/2019WR026085

Fernandez-Palomino, C.A., Hattermann, F.F., Krysanova, V., Vega-Jácome, F., Bronstert, A., 2020. Towards a more consistent eco-hydrological modelling through multi-objective calibration: a case study in the Andean Vilcanota River basin, Peru. Hydrological Sciences Journal 0, 1–16. https://doi.org/10.1080/02626667.2020.1846740

Ficklin, D.L., Barnhart, B.L., 2014. SWAT hydrologic model parameter uncertainty and its implications for hydroclimatic projections in snowmelt-dependent watersheds. Journal of Hydrology 519, 2081–2090. https://doi.org/10.1016/j.jhydrol.2014.09.082

Filoso, S., Bezerra, M.O., Weiss, K.C.B., Palmer, M.A., 2017. Impacts of forest restoration on water yield: A systematic review. PLoS One 12. https://doi.org/10.1371/journal.pone.0183210

Golden, H.E., Evenson, G.R., Tian, S., Amatya, D.M., Sun, G., 2016. Hydrological modelling in forested systems., in: Amatya, D.M., Williams, T.M., Bren, L., Jong, C. de (Eds.), Forest Hydrology: Processes, Management and Assessment. CABI, Wallingford, pp. 141–161. https://doi.org/10.1079/9781780646602.0141

Gorelick, N., Hancher, M., Dixon, M., Ilyushchenko, S., Thau, D., Moore, R., 2017. Google Earth Engine: Planetary-scale geospatial analysis for everyone. Remote Sensing of Environment, Big Remotely Sensed Data: tools, applications and experiences 202, 18–27. https://doi.org/10.1016/j.rse.2017.06.031

Gui Ziling, Liu Pan, Cheng Lei, Guo Shenglian, Wang Hao, Zhang Liping, 2019. Improving Runoff Prediction Using Remotely Sensed Actual Evapotranspiration during Rainless Periods. Journal of Hydrologic Engineering 24, 04019050. https://doi.org/10.1061/(ASCE)HE.1943-5584.0001856

Guo, T., Engel, B.A., Shao, G., Arnold, J.G., Srinivasan, R., Kiniry, J.R., 2018. Development and improvement of the simulation of woody bioenergy crops in the Soil and Water Assessment Tool (SWAT). Environmental Modelling & Software. https://doi.org/10.1016/j.envsoft.2018.08.030

Ha, L.T., Bastiaanssen, W.G.M., Van Griensven, A., Van Dijk, A.I.J.M., Senay, G.B., 2018. Calibration of Spatially Distributed Hydrological Processes and Model Parameters in SWAT Using Remote Sensing Data and an Auto-Calibration Procedure: A Case Study in a Vietnamese River Basin. Water 10, 212. https://doi.org/10.3390/w10020212

Haas, H., Dosdogru, F., Kalin, L., Yen, H., 2021a. Soft Data in Hydrologic Modeling: Prediction of Ecologically Relevant Flows with Alternate Land Use/Land Cover Data. Water 13, 2947. https://doi.org/10.3390/w13212947

969 Haas, H., Reaver, N.G.F., Karki, R., Kalin, L., Srivastava, P., Kaplan, D.A., Gonzalez-Benecke, C., 2021b.
970 Improving the representation of forests in hydrological models. Science of The Total
971 Environment 151425. https://doi.org/10.1016/j.scitotenv.2021.151425
972 Haas, M.B., Guse, B., Pfannerstill, M., Fohrer, N., 2016. A joined multi-metric calibration of river
973 discharge and nitrate loads with different performance measures. Journal of Hydrology 536,
974 534–545. https://doi.org/10.1016/j.jhydrol.2016.03.001
975 Hailegeorgis, T.T., Alfredsen, K., 2017. Analyses of extreme precipitation and runoff events including
976 uncertainties and reliability in design and management of urban water infrastructure. Journal of
977 Hydrology 544, 290–305. https://doi.org/10.1016/j.jhydrol.2016.11.037
978 Her, Y., Chaubey, I., 2015. Impact of the numbers of observations and calibration parameters on
979 equifinality, model performance, and output and parameter uncertainty. Hydrological Processes
980 29, 4220–4237. https://doi.org/10.1002/hyp.10487
981 Herman, M.R., Nejadhashemi, A.P., Abouali, M., Hernandez-Suarez, J.S., Daneshvar, F., Zhang, Z.,
982 Anderson, M.C., Sadeghi, A.M., Hain, C.R., Sharifi, A., 2018. Evaluating the role of
983 evapotranspiration remote sensing data in improving hydrological modeling predictability.
984 Journal of Hydrology 556, 39–49. https://doi.org/10.1016/j.jhydrol.2017.11.009
985 Himanshu, S.K., Pandey, A., Yadav, B., Gupta, A., 2019. Evaluation of best management practices for
986 sediment and nutrient loss control using SWAT model. Soil & Tillage Research 192, 42–58.
987 https://doi.org/10.1016/j.still.2019.04.016
988 Hernandez, A.J., Healey, S.P., Huang, H., Ramsey, R.D., 2018. Improved Prediction of Stream Flow Based
989 on Updating Land Cover Maps with Remotely Sensed Forest Change Detection. Forests 9, 317.
990 https://doi.org/10.3390/f9060317
991 Jensen, J.L.R., Humes, K.S., Hudak, A.T., Vierling, L.A., Delmelle, E., 2011. Evaluation of the MODIS LAI
992 product using independent lidar-derived LAI: A case study in mixed conifer forest. Remote
993 Sensing of Environment. 115: 3625-3639. 3625–3639. https://doi.org/10.1016/j.rse.2011.08.023
994 Jiang, D., Wang, K., 2019. The Role of Satellite-Based Remote Sensing in Improving Simulated
995 Streamflow: A Review. Water 11, 1615. https://doi.org/10.3390/w11081615
996 Jodar-Abellan, A., Valdes-Abellan, J., Pla, C., Gomariz-Castillo, F., 2018. Impact of land use changes on
997 flash flood prediction using a sub-daily SWAT model in five Mediterranean ungauged
998 watersheds (SE Spain) | Elsevier Enhanced Reader [WWW Document].
999 https://doi.org/10.1016/j.scitotenv.2018.12.034
1000 Kaur, B., Shrestha, N.K., Daggupati, P., Rudra, R.P., Goel, P.K., Shukla, R., Allataifeh, N., 2019. Water
1001 Security Assessment of the Grand River Watershed in Southwestern Ontario, Canada.
1002 Sustainability 11, 1883. https://doi.org/10.3390/su11071883
1003 Khaki, M., Hoteit, I., Kuhn, M., Forootan, E., Awange, J., 2019. Assessing data assimilation frameworks
1004 for using multi-mission satellite products in a hydrological context. Sci. Total Environ. 647, 1031–
1005 1043. https://doi.org/10.1016/j.scitotenv.2018.08.032
1006 Kiesel, J., Guse, B., Pfannerstill, M., Kakouei, K., Jähnig, S.C., Fohrer, N., 2017. Improving hydrological
1007 model optimization for riverine species. Ecological Indicators 80, 376–385.
1008 https://doi.org/10.1016/j.ecolind.2017.04.032
1009 Lai, G., Luo, J., Li, Q., Qiu, L., Pan, R., Zeng, X., Zhang, L., Yi, F., 2020. Modification and validation of the
1010 SWAT model based on multi-plant growth mode, a case study of the Meijiang River Basin, China.
1011 Journal of Hydrology 585, 124778. https://doi.org/10.1016/j.jhydrol.2020.124778
1012 Li, C., Sun, F., Xu, Y., Chen, T., Liu, M., Hu, Y., 2014. Combining CLUE-S and SWAT models to forecast land
1013 use change and non-point source pollution impact at a watershed scale in Liaoning Province,
1014 China. Chinese Geographical Science 24, 540–550. https://doi.org/10.1007/s11769-014-0661-x
1015 Li Zejun, Liu Pan, Feng Maoyuan, Cui Xueqing, He Ping, Wang Caijun, Zhang Jingwen, 2020. Evaluating
1016 the Effect of Transpiration in Hydrologic Model Simulation through Parameter Calibration.

Journal of Hydrologic Engineering 25, 04020007. https://doi.org/10.1061/(ASCE)HE.1943-5584.0001895
Lim, K.J., Engel, B.A., Tang, Z., Choi, J., Kim, K.-S., Muthukrishnan, S., Tripathy, D., 2005. AUTOMATED WEB GIS BASED HYDROGRAPH ANALYSIS TOOL, WHAT. J Am Water Resources Assoc 41, 1407–1416. https://doi.org/10.1111/j.1752-1688.2005.tb03808.x
Loizu, J., Massari, C., Álvarez-Mozos, J., Tarpanelli, A., Brocca, L., Casalí, J., 2018. On the assimilation set-up of ASCAT soil moisture data for improving streamflow catchment simulation. Advances in Water Resources 111, 86–104. https://doi.org/10.1016/j.advwatres.2017.10.034
Long, D., Longuevergne, L., Scanlon, B.R., 2014. Uncertainty in evapotranspiration from land surface modeling, remote sensing, and GRACE satellites. Water Resources Research 50, 1131–1151. https://doi.org/10.1002/2013WR014581
Ma, T., Duan, Z., Li, R., Song, X., 2019. Enhancing SWAT with remotely sensed LAI for improved modelling of ecohydrological process in subtropics. Journal of Hydrology 570, 802–815. https://doi.org/10.1016/j.jhydrol.2019.01.024
McLaughlin, D.L., Kaplan, D.A., Cohen, M.J., 2013. Managing Forests for Increased Regional Water Yield in the Southeastern U.S. Coastal Plain. JAWRA Journal of the American Water Resources Association 49, 953–965. https://doi.org/10.1111/jawr.12073
Mishra, A., Froebrich, J., Gassman, P.W., 2007. Evaluation of the Swat Model for Assessing Sediment Control Structures in a Small Watershed in India. Transactions of the ASABE 50, 469–477. https://doi.org/10.13031/2013.22637
Monteith, J.L., 1965. Evaporation and environment. Symposia of the Society for Experimental Biology 19, 205–234.
Moriasi, D.N., Gitau, M.W., Pai, N., Daggupati, P., 2015. Hydrologic and Water Quality Models: Performance Measures and Evaluation Criteria.
Mwangi, H.M., Julich, S., Patil, S.D., McDonald, M.A., Feger, K.-H., 2016. Modelling the impact of agroforestry on hydrology of Mara River Basin in East Africa - Mwangi - 2016 - Hydrological Processes - Wiley Online Library [WWW Document]. Hydrological Processes. URL https://onlinelibrary.wiley.com/doi/full/10.1002/hyp.10852 (accessed 9.24.19).
Myneni, R., Knyazikhin, Y., 2015. MOD15A2H MODIS/Terra Leaf Area Index/FPAR 8-Day L4 Global 500m SIN Grid V006. https://doi.org/10.5067/modis/mod15a2h.006
Neitsch, S.L., Arnold, J.G., Kiniry, J.R., Williams, J.R., 2011. Soil and water assessment tool theoretical documentation: version 2009. Texas Water Resources Institute Technical Report No. 406. Texas Water Resources Institute, USA.
Odusanya, A.E., Mehdi, B., Schürz, C., Oke, A.O., Awokola, O.S., Awomeso, J.A., Adejuwon, J.O., Schulz, K., 2019. Multi-site calibration and validation of SWAT with satellite-based evapotranspiration in a data-sparse catchment in southwestern Nigeria. Hydrology and Earth System Sciences 23, 1113–1144. https://doi.org/10.5194/hess-23-1113-2019
Parajuli, P.B., Jayakody, P., Ouyang, Y., 2018. Evaluation of Using Remote Sensing Evapotranspiration Data in SWAT. Water Resour Manage 32, 985–996. https://doi.org/10.1007/s11269-017-1850-z
Pregnolato, M., Ford, A., Robson, C., Glenis, V., Barr, S., Dawson, R., 2016. Assessing urban strategies for reducing the impacts of extreme weather on infrastructure networks. R Soc Open Sci 3, 160023. https://doi.org/10.1098/rsos.160023
Rajib, A., Evenson, G.R., Golden, H.E., Lane, C.R., 2018. Hydrologic model predictability improves with spatially explicit calibration using remotely sensed evapotranspiration and biophysical parameters. Journal of Hydrology 567, 668–683. https://doi.org/10.1016/j.jhydrol.2018.10.024
Rajib, A., Merwade, V., Yu, Z., 2018b. Rationale and Efficacy of Assimilating Remotely Sensed Potential Evapotranspiration for Reduced Uncertainty of Hydrologic Models. Water Resources Research 54, 4615–4637. https://doi.org/10.1029/2017WR021147

Rajib, M.A., Merwade, V., Yu, Z., 2016. Multi-objective calibration of a hydrologic model using spatially distributed remotely sensed/in-situ soil moisture. Journal of Hydrology 536, 192–207. https://doi.org/10.1016/j.jhydrol.2016.02.037

Rajib, A., Kim, I.L., Golden, H.E., Lane, C.R., Kumar, S.V., Yu, Z., Jeyalakshmi, S., 2020. Watershed Modeling with Remotely Sensed Big Data: MODIS Leaf Area Index Improves Hydrology and Water Quality Predictions. Remote Sensing 12, 2148. https://doi.org/10.3390/rs12132148

Ramesh, R., Anderson, C.J., Kalin, L., 2020. Characterizing nitrogen attenuation by headwater slope wetlands across different land uses. Ecological Engineering 149, 105833. https://doi.org/10.1016/j.ecoleng.2020.105833

Richter, B.D., Baumgartner, J.V., Powell, J., Braun, D.P., 1996. A Method for Assessing Hydrologic Alteration within Ecosystems. Conservation Biology 10, 1163–1174. https://doi.org/10.1046/j.1523-1739.1996.10041163.x

Romanowicz, A. a., Vanclooster, M., Rounsevell, M., La Junesse, I., 2005. Sensitivity of the SWAT model to the soil and land use data parametrisation: a case study in the Thyle catchment, Belgium. Ecological Modelling 187, 27–39. https://doi.org/10.1016/j.ecolmodel.2005.01.025

Ruefenacht, B., Finco, M.V., Nelson, M.D., Czaplewski, R., Helmer, E.H., Blackard, J.A., Holden, G.R., Lister, A.J., Salajanu, D., Weyermann, D., Winterberger, K., 2008. Conterminous U.S. and Alaska Forest Type Mapping Using Forest Inventory and Analysis Data. photogramm eng remote sensing 74, 1379–1388. https://doi.org/10.14358/PERS.74.11.1379

Running, S., Mu, Q., 2017. MOD16A2 MODIS/Terra Net Evapotranspiration 8-Day L4 Global 500m SIN Grid V006. https://doi.org/10.5067/modis/mod16a2.006

Sengupta, M., Xie, Y., Lopez, A., Habte, A., Maclaurin, G., Shelby, J., 2018. The National Solar Radiation Data Base (NSRDB). Renewable and Sustainable Energy Reviews 89, 51–60. https://doi.org/10.1016/j.rser.2018.03.003

Shen, Z.Y., Chen, L., Chen, T., 2012. Analysis of parameter uncertainty in hydrological and sediment modeling using GLUE method: a case study of SWAT model applied to Three Gorges Reservoir Region, China. Hydrology and Earth System Sciences 16, 121–132. https://doi.org/10.5194/hess-16-121-2012

Strauch, M., Volk, M., 2013. SWAT plant growth modification for improved modeling of perennial vegetation in the tropics. Ecological Modelling 269, 98–112. https://doi.org/10.1016/j.ecolmodel.2013.08.013

Sun, G., McNulty, S.G., Lu, J., Amatya, D.M., Liang, Y., Kolka, R.K., 2005. Regional annual water yield from forest lands and its response to potential deforestation across the southeastern United States. Journal of Hydrology 308 (2005) 258-268.

Sun, G., Alstad, K., Chen, J., Chen, S., Ford, C.R., Lin, G., Liu, C., Lu, N., McNulty, S.G., Miao, H., Noormets, A., Vose, J.M., Wilske, B., Zeppel, M., Zhang, Y., Zhang, Z., 2011. A general predictive model for estimating monthly ecosystem evapotranspiration. Ecohydrology 4, 245–255. https://doi.org/10.1002/eco.194

Tabacchi, E., Lambs, L., Guilloy, H., Planty-Tabacchi, A.-M., Muller, E., Décamps, H., 2000. Impacts of riparian vegetation on hydrological processes. Hydrological Processes 14, 2959–2976. https://doi.org/10.1002/1099-1085(200011/12)14:16/17<2959::AID-HYP129>3.0.CO;2-B

Tague, C.L., Band, L.E., 2001. Evaluating explicit and implicit routing for watershed hydro-ecological models of forest hydrology at the small catchment scale. Hydrological Processes 15, 1415–1439. https://doi.org/10.1002/hyp.171

Teklay, A., Dile, Y.T., Setegn, S.G., Demissie, S.S., Asfaw, D.H., 2019. Evaluation of static and dynamic land use data for watershed hydrologic process simulation: A case study in Gummara watershed, Ethiopia. CATENA 172, 65–75. https://doi.org/10.1016/j.catena.2018.08.013

TNC, 2009. The Nature Conservancy, 2009. Indicators of Hydrologic Alteration Version 7.1 User's Manual. Available at: https://www.conservationgateway.org/Documents/IHAV7.pdf (accessed on 09/01/2020).

Tobin, K.J., Bennett, M.E., 2017. Constraining SWAT Calibration with Remotely Sensed Evapotranspiration Data. JAWRA Journal of the American Water Resources Association 53, 593–604. https://doi.org/10.1111/1752-1688.12516

Wang, Q., Liu, R., Men, C., Guo, L., Miao, Y., 2018. Effects of dynamic land use inputs on improvement of SWAT model performance and uncertainty analysis of outputs. Journal of Hydrology 563, 874–886. https://doi.org/10.1016/j.jhydrol.2018.06.063

Wang, R., Kalin, L., 2018. Combined and synergistic effects of climate change and urbanization on water quality in the Wolf Bay watershed, southern Alabama. Journal of Environmental Sciences 64, 107–121. https://doi.org/10.1016/j.jes.2016.11.021

Watson, B., Coops, N., Selvalingam, S., Ghafouri, M., 2005. Integration of 3-PG into SWAT to simulate the growth of evergreen forests. SWAT 2005 : 3rd International SWAT Conference 142–152.

Wheater, H., Evans, E., 2009. Land use, water management and future flood risk. Land Use Policy, Land Use Futures 26, S251–S264. https://doi.org/10.1016/j.landusepol.2009.08.019

Williams, C.A., Reichstein, M., Buchmann, N., Baldocchi, D., Beer, C., Schwalm, C., Wohlfahrt, G., Hasler, N., Bernhofer, C., Foken, T., Papale, D., Schymanski, S., Schaefer, K., 2012. Climate and vegetation controls on the surface water balance: Synthesis of evapotranspiration measured across a global network of flux towers. Water Resources Research 48. https://doi.org/10.1029/2011WR011586

Williams, J.R., 1975. Sediment Routing for Agricultural Watersheds1. JAWRA Journal of the American Water Resources Association 11, 965–974. https://doi.org/10.1111/j.1752-1688.1975.tb01817.x

Williams, J.R., 1990. The erosion-productivity impact calculator (EPIC) model: a case history. Phil. Trans. R. Soc. Lond. B 329, 421–428. https://doi.org/10.1098/rstb.1990.0184

Wit, M.J.M. de, 2001. Nutrient fluxes at the river basin scale. I: the PolFlow model. Hydrological Processes 15, 743–759. https://doi.org/10.1002/hyp.175

Yang, Q., Almendinger, J.E., Zhang, X., Huang, M., Chen, X., Leng, G., Zhou, Y., Zhao, K., Asrar, G.R., Srinivasan, R., Li, X., 2018. Enhancing SWAT simulation of forest ecosystems for water resource assessment: A case study in the St. Croix River basin. Ecological Engineering 120, 422–431. https://doi.org/10.1016/j.ecoleng.2018.06.020

Yang, Q., Zhang, X., 2016. Improving SWAT for simulating water and carbon fluxes of forest ecosystems. Science of The Total Environment 569–570, 1478–1488. https://doi.org/10.1016/j.scitotenv.2016.06.238

Zhang, H., Wang, B., Liu, D.L., Zhang, M., Leslie, L.M., Yu, Q., 2020. Using an improved SWAT model to simulate hydrological responses to land use change: A case study of a catchment in tropical Australia. Journal of Hydrology 585, 124822. https://doi.org/10.1016/j.jhydrol.2020.124822

Zhang, X., Jin, C., Guan, D., Wang, A., Wu, J., Yuan, F., 2012. Long-Term Eddy Covariance Monitoring of Evapotranspiration and Its Environmental Factors in a Temperate Mixed Forest in Northeast China. Journal of Hydrologic Engineering 17, 965–974. https://doi.org/10.1061/(ASCE)HE.1943-5584.0000549

Zhang, Y., Chiew, F.H.S., Liu, C., Tang, Q., Xia, J., Tian, J., Kong, D., Li, C., 2020. Can Remotely Sensed Actual Evapotranspiration Facilitate Hydrological Prediction in Ungauged Regions Without Runoff Calibration? Water Resources Research 56, e2019WR026236. https://doi.org/10.1029/2019WR026236

Zhang, Y., Sun, A., Sun, H., Gui, D., Xue, J., Liao, W., Yan, D., Zhao, N., Zeng, X., 2019. Error adjustment of TMPA satellite precipitation estimates and assessment of their hydrological utility in the middle

and upper Yangtze River Basin, China. Atmospheric Research 216, 52–64. https://doi.org/10.1016/j.atmosres.2018.09.021

Ziemer, R.R., Lewis, J., Rice, R.M., Lisle, T.E., 1991. Modeling the cumulative watershed effects of forest management strategies. Journal of Environmental Quality 20(1): 36-42.